Antagonism of the mammalian target of rapamycin selectively mediates metabolic effects of epidermal growth factor receptor inhibition and protects human malignant glioma cells from hypoxia-induced cell death

Ronellenfitsch, M W ; Brucker, D P ; Burger, M C ; Wolking, S ; Tritschler, F ; Rieger, J ; Wick, W ; Weller, M ; Steinbach, J P

Abstract: Although inhibition of the epidermal growth factor receptor is a plausible therapy for malignant gliomas that, in vitro, enhances apoptosis, the results of clinical trials have been disappointing. The mammalian target of rapamycin (mTOR) is a serine/threonine kinase that integrates starvation signals and generates adaptive responses that aim at the maintenance of energy homeostasis. Antagonism of mTOR has been suggested as a strategy to augment the efficacy of epidermal growth factor receptor inhibition by interfering with deregulated signalling cascades downstream of Akt. Here we compared effects of antagonism of mTOR utilizing rapamycin or a small hairpin RNA-mediated gene silencing to those of epidermal growth factor receptor inhibition or combined inhibition of epidermal growth factor receptor and mTOR in human malignant glioma cells. In contrast to epidermal growth factor receptor inhibition, mTOR antagonism neither induced cell death nor enhanced apoptosis induced by CD95 ligand or chemotherapeutic drugs. However, mTOR inhibition mimicked the hypoxia-protective effects of epidermal growth factor receptor inhibition by maintaining adenosine triphosphate levels. These in vitro experiments thus challenge the current view of mTOR as a downstream target of Akt that mediates anti-apoptotic stimuli. Under the conditions of the tumour microenvironment, metabolic effects of inhibition of epidermal growth factor receptor, Akt and mTOR may adversely affect outcome by protecting the hypoxic tumour cell fraction.

DOI: https://doi.org/10.1093/brain/awp093

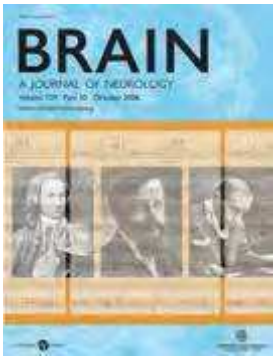

Antagonism of mTOR selectively mediates metabolic effects of EGFR inhibition and protects human malignant glioma cells from hypoxia-induced cell death

Journal:	*Brain*
Manuscript ID:	BRAIN-2008-01390.R2
Manuscript Type:	Original Paper
Date Submitted by the Author:	
Complete List of Authors:	Ronellenfitsch, Michael; University of Tübingen, Medical School, Laboratory for Molecular Neurooncology, Department of General Neurology; Goethe-University Hospital, Dr. Senckenberg Institute of Neurooncology, Center of Neurology and Neurosurgery Brucker, Daniel; Goethe-University Hospital, Dr. Senckenberg Institute of Neurooncology, Center of Neurology and Neurosurgery Burger, Michael; Goethe-University Hospital, Dr. Senckenberg Institute of Neurooncology, Center of Neurology and Neurosurgery Wolking, Stefan; University of Tübingen, Medical School, Laboratory for Molecular Neurooncology, Department of General Neurology Tritschler, Felix; University of Tübingen, Medical School, Laboratory for Molecular Neurooncology, Department of General Neurology Rieger, Johannes; Goethe-University Hospital, Dr. Senckenberg Institute of Neurooncology, Center of Neurology and Neurosurgery Wick, Wolfgang; German Cancer Research Center, Clinical Cooperation Unit Neurooncology Weller, Michael; University Hospital Zürich, Department of Neurology Steinbach, Joachim; Goethe-University Hospital, Dr. Senckenberg Institute of Neurooncology, Center of Neurology and Neurosurgery
Key Words:	
Please choose up to 5	mTOR, glioma, metabolism, EGFR, hypoxia

Manuscript title

Antagonism of mTOR selectively mediates metabolic effects of EGFR inhibition and protects human malignant glioma cells from hypoxia-induced cell death

Michael W. Ronellenfitsch[1,2], Daniel P. Brucker[2], Michael C. Burger[2], Stefan Wolking[1], Felix Tritschler[1], Johannes Rieger[2], Wolfgang Wick[3], Michael Weller[1,4] and Joachim P. Steinbach[2,*]

*Corresponding author, Phone: +49 (0)69 6301 87711, Fax: +49 (0)69 6301 87713, Email: joachim.steinbach@med.uni-frankfurt.de

[1]Laboratory for Molecular Neurooncology
Department of General Neurology
University of Tübingen, Medical School
Hoppe-Seyler-Strasse 3
72076 Tübingen
Germany

[2]Dr. Senckenberg Institute of Neurooncology
Center of Neurology and Neurosurgery
Goethe-University Hospital
Schleusenweg 2-16
60528 Frankfurt am Main
Germany

[3]German Cancer Research Center

Clinical Cooperation Unit Neurooncology

Im Neuenheimer Feld 280

69120 Heidelberg

Germany

[4]Department of Neurology

University Hospital Zürich

Frauenklinikstrasse 26

8091 Zürich

Switzerland

Running title

mTOR antagonism in malignant glioma cells

Abstract

Although inhibition of the epidermal growth factor receptor (EGFR) is a plausible therapy for malignant gliomas that, in vitro, enhances apoptosis, the results of clinical trials have been disappointing. The mammalian target of rapamycin (mTOR) is a serine/threonine kinase that integrates starvation signals and generates adaptive responses that aim at the maintenance of energy homeostasis. Antagonism of mTOR has been suggested as a strategy to augment the efficacy of EGFR inhibition by interfering with deregulated signalling cascades downstream of Akt. Here we compared effects of antagonism of mTOR utilizing rapamycin or small hairpin RNA (shRNA)-mediated gene silencing to those of EGFR inhibition or combined inhibition of EGFR and mTOR in human malignant glioma cells. In contrast to EGFR inhibition, mTOR antagonism neither induced cell death nor enhanced apoptosis induced by CD95 ligand (CD95L) or chemotherapeutic drugs. However, mTOR inhibition mimicked the hypoxia-protective effects of EGFR inhibition by maintaining ATP levels. These in vitro experiments thus challenge the current view of mTOR as a downstream target of Akt that mediates antiapoptotic stimuli. Under the conditions of the tumour microenvironment, metabolic effects of inhibition of EGFR, Akt and mTOR may adversely affect outcome by protecting the hypoxic tumour cell fraction.

Abstract: 198 words

Key words: mTOR, EGFR, glioma, hypoxia, metabolism

Abbreviations:

4E-BP1, eukaryotic translation initiation factor 4E binding protein 1

CD95L, CD95 ligand

EGFR, epidermal growth factor receptor

eIF4E, eukaryotic translation initiation factor 4E

HIF-1 α, hypoxia inducible factor-1 α

LDH, lactate dehydrogenase

mTOR, mammalian target of rapamycin

p42/44 MAPK, p42/44 mitogen-activated protein kinase

PI3K, phosphatidyl-inositole-3-phosphate kinase

RPS6, ribosomal protein S6

S6K1, ribosomal protein S6 kinase 1

shRNA, small hairpin RNA

Deleted: CD95L, CD95 ligand¶
PI3K, phosphatidyl-inositole-3-phosphate kinase¶
eIF4E, eukaryotic translation initiation factor 4E¶
4E-BP1, eukaryotic translation initiation factor 4E binding protein 1¶
S6K1, ribosomal protein S6 kinase 1¶
RPS6, ribosomal protein S6¶
p42/44 MAPK, p42/44 mitogen-activated protein kinase¶
HIF-1 α, hypoxia inducible factor-1 α¶
LDH, lactate dehydrogenase¶

Deleted: Key words: mTOR, EGFR, glioma, hypoxia, metabolism¶

Introduction

Patients with glioblastoma face a grim prognosis with a median survival of less than one year in unselected cohorts (Ohgaki et al., 2004). Novel therapeutic approaches are therefore urgently needed. Targeting signalling downstream of activated growth factor receptors is currently considered one of the most promising approaches. Specifically, the EGFR is amplified or activated in the majority of primary glioblastomas and can be regarded as one of the most plausible targets for molecular therapy (Kleihues et al., 2000). EGFR signalling sustains many key features of the neoplastic phenotype, e.g. it enhances cell autonomous growth, invasion and angiogenesis and confers protection from growth inhibitory and proapoptotic stimuli (Mendelsohn, 2002; Steinbach and Weller, 2002).

Clinical trials with small molecule kinase inhibitors of the EGFR in malignant glioma patients, however, have produced disappointing results (Van Den Bent et al., 2007). Insufficient suppression of the intracellular signalling cascade downstream of EGFR has been suggested as an important cause for the failure of EGFR inhibitors. Phosphorylation of Akt, in particular, represents a negative predictive marker for the response of malignant glioma patients to EGFR inhibitors (Haas-Kogan et al., 2005). The serine/threonine kinase mTOR is a key mediator of phosphatidyl-inositole-3-phosphate kinase (PI3K) and Akt signalling. It integrates growth-inhibitory signals such as deprivation of glucose and amino acids, ATP depletion, hypoxia and lack of growth factors (Wullschleger et al., 2006) in order to generate adaptive cellular responses primarily by altering the translation of specific proteins. Deregulated mTOR signalling sustains proliferation of malignant cells by antagonizing these physiological starvation signals (Peng et al., 2002). It therefore appears plausible that the commonly observed activation of mTOR signalling in glioblastoma (Choe et al.,

2003) contributes to the typical pattern of glioblastoma pathology with necrotic cores and aggressive growth at the tumour margins. The translational effects of mTOR signalling are mediated by phosphorylation of its two direct target molecules, eukaryotic translation initiation factor 4E binding protein 1 (4E-BP1) and ribosomal protein S6 kinase 1 (S6K1), at specific sites. Phosphorylation of 4E-BP1 occurs stepwise and relieves its repression of eukaryotic initiation factor 4E (eIF4E) (Hara et al., 1997), resulting in activation of translation initiation. In this process, phosphorylation of the residues Thr37/46 is the initial step in 4E-BP1 phosphorylation. It is also a prerequisite for phosphorylation of residues Thr70 and Ser65, whose phosphorylation alone is not sufficient to block binding to eIF4E (Gingras et al., 2001). The different phosphorylation states of 4E-BP1 are evidenced by 3 differently migrating bands in immunoblot analyses: a fastest migrating hypophosphorylated α band, a β band of intermediate mobility and a slowest migrating hyperphosphorylated γ band. Thr37/46 phosphorylated 4E-BP1 can be detected in all 3 bands and is relatively insensitive to serum deprivation and mTOR inhibition. However, the pattern of phosphorylated 4E-BP1 shifts to the hypophosphorylated faster migrating bands following mTOR inhibition (Brunn et al., 1997). Phosphorylation of S6K1 results in activation of its kinase activity and phosphorylation of ribosomal protein S6 (RPS6), which, among other proteins, regulates translation of ribosomal proteins and elongation factors (Hay and Sonenberg, 2004). With the availability of rapamycin and related drugs that specifically inhibit mTOR signalling, considerable interest has been generated to investigate antagonism of mTOR as an anti-glioma strategy (Hidalgo and Rowinsky, 2000; Huang and Houghton, 2001). In preclinical models, mTOR inhibition has been reported to result in apoptotic and non-apoptotic cell death (Rao et al., 2005; Takeuchi et al., 2005), cell cycle arrest (Tanaka et al., 2007) and

Deleted: first

decreased angiogenesis (Del Bufalo et al., 2006). mTOR inhibition is particularly effective against some cell lines with mutant PTEN (Neshat et al., 2001). Augmentation of the efficacy of EGFR inhibition by mTOR inhibition therefore appears plausible (Doherty et al., 2006; Reardon et al., 2006). However, we have previously identified an undesirable consequence of interference with EGFR function that offers an alternative explanation for the poor clinical performance of EGFR antagonistic strategies and may also adversely affect the efficacy of mTOR inhibition. Altered cellular metabolism and energy expenditure, which are enhanced by EGFR signalling, are at the core of this phenomenon which results in the protection of malignant glioma cells from hypoxia when EGFR is inhibited (Steinbach et al., 2004; Steinbach et al., 2005). In these experiments, EGFR inhibition and resistance towards hypoxia were associated with decreased phosphorylation of the mTOR target RPS6. Given the physiological role of mTOR in the regulation of metabolic demands, these results suggested that EGFR inhibition confers protection against hypoxia in a mTOR-dependent fashion. We here report the results of a comprehensive analysis of cell-autonomous effects of mTOR antagonism on CD95L-, chemotherapy- and hypoxia-induced cell death in human malignant glioma cells employing rapamycin and shRNA-mediated gene suppression of mTOR (Brummelkamp et al., 2002) and a comparison of mTOR inhibition with EGFR inhibition or combined inhibition of mTOR and EGFR.

Materials and Methods

Reagents and cell lines

U0126, an inhibitor of MEK 1 and 2, the PI3K inhibitor LY294002, Akt inhibitor VIII and EGF were purchased from Calbiochem (San Diego, CA, USA), the EGFR inhibitor PD153035 and the mTOR inhibitor rapamycin from Tocris Cookson (Bristol, UK), erlotinib and IGF-1 from Roche (Mannheim, Germany). Tumour necrosis factor-related apoptosis-inducing ligand (TRAIL) was purchased from PeproTech (Rocky Hill, NJ, USA). LNT-229 (PTEN wildtype) and U87MG (PTEN mutant) human malignant glioma cell lines have been described (Ishii et al., 1999; Steinbach et al., 2004; Steinbach et al., 2003). The generation of primary cell cultures has also been previously described (Bahr et al., 2003). Established glioma cell lines and primary cultures were maintained in Dulbecco's modified eagle medium (DMEM) containing 10% foetal calf serum (FCS) (Biochrom KG, Berlin, Germany), 100 IU/ml penicillin and 100 mg/ml streptomycin (Life Technologies, Karlsruhe, Germany). pSUPER puro transfected cells were maintained in medium containing 2 µg/ml puromycin (Sigma, Deisenhofen, Germany). Lomustine (CCNU, 1-[2-chloroethyl]-3-cyclohexyl-1-nitrosourea) and vincristine as well as all other chemicals not specified below were purchased from Sigma.

Immunoblot analysis

Immediately after incubation, cells were washed with ice-cold PBS and harvested into ice-cold PBS containing protease inhibitors. Cellular lysates were prepared as described (Steinbach et al., 2003) and subjected to SDS-PAGE analysis. Membranes were probed with antibodies to phospho-p90^{RSK} (P-p90^{RSK}) (Ser380), phospho-Akt (P-Akt) (Ser473), phospho-p42/44 mitogen-activated protein kinase (P-p42/44 MAPK)

(Thr202/Tyr204), phospho-RPS6 (P-RPS6) (Ser235/236) and eIF4E (employed here as internal standard for equal protein loading) utilizing the Pathscan Multiplex Western Cocktail I or with antibodies to P-Akt (Ser473), Akt, P-p42/44 MAPK (Thr202/Tyr204), phospho-S6K1 (P-S6K1) (Thr389), S6K1, phospho-4E-BP1 (P-4E-BP1) (Thr37/46), 4E-BP1 and mTOR all purchased from Cell Signaling (Beverly, MA, USA). The antibody to hypoxia inducible factor (HIF)-1 α was purchased from R&D Systems (Minneapolis, MN, USA) and the antibody to cyclin D1 and p42/44 MAPK was from Santa Cruz Biotechnology (Santa Cruz, Ca, USA). The secondary anti-rabbit and anti-goat antibodies were purchased from Santa Cruz Biotechnology. Enhanced chemiluminescence (ECL+) (Amersham, Little Chalfont, UK) was used for detection.

Cell growth and viability assays

Cell growth was assessed by crystal violet staining as previously described (Roth et al., 1997). Further cultures derived from primary glioblastoma surgery specimens were pulsed with [methyl-^{3}H]thymidine (1 µCi; Amersham) on day 2 and collected 16 h later using a cell harvester (Tomtec, Hamden, CT). Incorporated radioactivity was bound to a glass fiber filtermat (Wallac, Turku, Finland). The filtermat was wetted with Ultima Gold Scintillation Cocktail (Packard, Dreieich, Germany) and radioactivity was determined in a Wallac 1450 Microbeta Plus Liquid Scintillation Counter. For cell viability analysis, the cells were washed with ice-cold PBS, stained with 5 µg/ml propidium iodide (PI) in PBS and analysed by flow cytometry employing a DAKO CyAn flow cytometer and Summit 4.2. software. Alternatively, cell viability was analysed by lactate dehydrogenase (LDH) release assays (Steinbach et al., 2004). CD95L was obtained from the supernatant of CD95L-transfected N2A murine neuroblastoma cells (Roth et al., 1997). For the detection of chemotherapy-induced

cell death, the cells were plated on 96 well plates (Falcon, Becton-Dickinson) at 1.5 x 10^4/well and allowed to attach overnight. Then the cells were incubated with or without rapamycin and chemotherapeutics for 72 h in serum-free medium and stained with crystal violet.

Induction of hypoxia

Hypoxia was induced by incubating cells in Gas Pak pouches for anaerobic culture (Becton Dickinson, Heidelberg, Germany) (Steinbach et al., 2003). Briefly, the cells were plated on 96 well plates at 2 x 10^4/well or petri dishes of various sizes and allowed to attach overnight. Then the cells were incubated in serum-free DMEM without glucose (Gibco BRL, Basel, Switzerland) adjusted to 2 mM glucose under normoxia or hypoxia for the indicated time periods. Equal cell densities were ensured by crystal violet staining when comparing vehicle and rapamycin pre-incubated cells as wells as LNT-229 puro and LNT-229 mTORsh cells.

Generation of LNT-229 mTORsh knockdown cells

The pSUPER plasmid was obtained from R. Agami (Amsterdam, The Netherlands). A puromycin cassette was inserted into the NaeI site. The mTOR-specific oligonucleotide sequences GATCCCC **ACTTCGAAGCTGTGCTACA** ttcaagaga **TGTAGCACAGCTTCGAAGT** TTTTTGGAAA and TCGATTTCCAAAAA **ACTTCGAAGCTGTGCTACA** tctcttgaa **TGTAGCACAGCTTCGAAGT** GGG [nucleotides (nt) 5,469-5,487] were obtained from Biomers.net (Ulm, Germany) and cloned into the BglII and SalI sites of pSUPER. The mTOR-specific parts of the sequences are underlined. For the generation of stable mTORsh transfectants, pSUPER puro control or mTORsh plasmids were introduced using FuGene6 transfection reagent (Roche).

ATP assay

Immediately after normoxic or hypoxic incubation, the plates were placed on ice and the cells were pelleted by centrifugation and lysed in ATP releasing reagent (Sigma). The ATP concentration was determined by luciferase assay with the CLS II kit (Boehringer, Mannheim, Germany) (Steinbach et al., 2003).

JC-1 assay

Following treatment as indicated, the cells were washed in PBS and incubated for 15 min in JC-1 staining reagent (Biocarta, Hamburg, Germany) at 37°C. Then the cells were washed once in assay buffer, resuspended in PBS and analysed by flow cytometry.

Glucose assay

Immediately after hypoxia the cells were pelleted by centrifugation and the supernatant was assayed for glucose employing the Gluco-quant kit (Roche).

Statistical analysis

Quantitative data obtained for cell density by crystal violet, LDH-release, glucose and ATP concentrations are expressed as mean and SD as indicated. *P*-values for cell density by crystal violet, LDH-release, glucose and ATP concentration were derived from two-tailed Student's *t*-tests. Values of $P > 0.05$ were considered not significant (n.s.), values of $P < 0.05$ and $P < 0.01$ were considered significant and highly significant (Excel, Microsoft, Seattle, WA, USA). When multiple tests were performed significance levels (α values) were adjusted using the Holm-Bonferroni method.

Results

Preferential inhibition of the p70 isoform of S6K1 by rapamycin in human malignant glioma cells

To establish the specific pattern of rapamycin action in human malignant glioma cells, PTEN wildtype LNT-229 or PTEN mutant U87MG cells were exposed to rapamycin. Phosphorylation of the 70 kD isoform of the direct mTOR target S6K1, which correlates with its activity (Harris and Lawrence, 2003), was inhibited by rapamycin in a concentration-dependent fashion and abolished at a concentration of 100 nM in both cell lines (Fig. 1). Therefore, this concentration which also corresponds to the effective rapamycin concentrations required in other malignant glioma and non-glioma cell lines (Peng et al., 2002; Tanaka et al., 2007; Wei et al., 2008), was used as a standard for subsequent experiments. Of note, the 85 kD isoform of S6K1 which is located in the nucleus and known to be less abundant than the 70 kD isoform in some cell lines (Reinhard et al., 1994), was much less sensitive to inhibition by rapamycin, particularly in U87MG cells.

CD95L- and chemotherapy-induced cell death: dissociation of the effects of EGFR inhibition and mTOR inhibition

EGFR-dependent signalling is a major determinant of susceptibility towards death ligand/CD95L- and chemotherapy-induced cell death in human malignant glioma cells. It has been suggested that the proapoptotic properties of EGFR inhibitors are mediated by decreased mTOR signalling. To compare the effects of mTOR inhibition with those of inhibition of EGFR, PI3K or MEK, LNT-229 and U87MG cells were exposed to rapamycin, PD153035, LY294002 and U0126 alone or in combination.

The specificity of pathway inhibition was assessed by immunoblot analysis for phosphorylated $p90^{RSK}$, Akt, p42/44 MAPK, RPS6, 4E-BP1 and total eIF4E or 4E-BP1 as a loading control (Fig. 2A). In PTEN wildtype LNT-229 cells, only the EGFR inhibitor PD153035 abolished RPS6 phosphorylation when administered alone (Fig. 2A). In contrast, rapamycin, LY294002 and U0126 only partially inhibited the phosphorylation of RPS6. Co-inhibition of PI3K and MEK with LY294002 and U0126 mimicked the effects of PD153035 on P-RPS6, suggesting that both branches of EGFR signalling, PI3K and MEK, must be inhibited for abrogation of RPS6 phosphorylation. Accordingly, RPS6 phosphorylation was still detectable, albeit at a much lower level, in S6K knockout cells (Pende et al., 2004) and RPS6 can also be phosphorylated by $p90^{RSK}$ (Roux et al., 2007). Thus, dual mechanisms originating from MEK as well as from mTOR regulate the indirect mTOR target RPS6. In U87MG cells, rapamycin was the most effective agent for RPS6 inhibition, whereas PD153035 and U0126 had no effect (Fig. 2A). The inefficient inhibition of RPS6 phosphorylation by PD153035 is plausible given that U87MG cells lack functional PTEN (Ishii et al., 1999). No agent alone abrogated Thr37/46 4E-BP1 phosphorylation with roughly equivalent effects of rapamycin, PD153035 and LY294002 in LNT-229 and of rapamycin and LY294002 in U87MG cells. The most pronounced effects on 4E-BP1 phosphorylation were achieved by combining rapamycin with PD153035 or LY294002 and the effect of these inhibitors was most pronounced in the slowest migrating γ band of 4E-BP1.

The cell death-promoting potential of mTOR inhibition was then assessed by exposing LNT-229 or U87MG cells to CD95L in the presence of rapamycin, PD153035, LY294002 or U0126 alone or combined as indicated. (Fig. 2A, lower panel). Rapamycin alone sensitized neither LNT-229 nor U87MG cells to CD95L. Rapamycin also failed to induce synergistic or additive cytotoxic effects when

combined with PD153035, LY294002 or U0126 (Fig. 2A, bottom panel). In LNT-229 cells PD153035 was the only agent which substantially sensitized to CD95L. While both substances alone did not modulate CD95L-induced cell death, the combination of LY294002 and U0126 also sensitized the cells, although to a lesser degree than PD153035. Notably, also the combination of rapamycin with U0126 which abolished RPS6 phosphorylation in the immunoblot analysis was inefficient. Largely similar results were obtained in U87MG cells (Fig. 2A, bottom panel) with PD153035 as the most potent sensitising agent and rapamycin failing to show any effect alone or in any of the investigated combinations. Although after correction for multiple testing only PD153035, PD153035 plus rapamycin and LY294002 plus U0126 achieved significance in U87MG cells. In parallel experiments with LNT-229 and U87MG cells, CD95L-induced cell death in the presence of rapamycin or PD513035 was analysed by LDH release with similar results, indicating that the CD95L-mediated effect is not due to an inhibition of proliferation rather than cell death (data not shown). Since mTOR exerts its effect partially through modulation of mRNA translation, we asked whether pretreatment of glioma cells with rapamycin, to allow for the time necessary to reach the new levels of target proteins, alters susceptibility to CD95L-mediated apoptosis. Again, rapamycin was ineffective (data not shown). Notably, exposure to rapamycin up to 24 h did not induce growth inhibition or cell death in any of these experiments as assessed by crystal violet staining or LDH release assays.

Concerning inhibitor specificity, we have previously shown that the EGFR inhibitor AG1478 has similar effects as PD153035 both with regard to sensitivity to apoptosis (Steinbach et al., 2002) and protection from hypoxia-induced cell death (Steinbach et al., 2004). To delineate consequences for clinical practise, we performed additional experiments with the clinically used EGFR inhibitor erlotinib (supplementary Fig. S1A), We also performed experiments with lower inhibitor concentrations of the PI3K

and MEK inhibitors (5 µM LY294002 and 10 µM U0126) since their necessary concentrations remain controversial, with similar results (compare Fig. 2A and supplementary Fig. S1C).

To further clarify the level of EGFR-dependent signal transduction that mediates the proapoptotic consequences, we performed experiments with the Akt-specific inhibitor Akt inhibitor VIII which blocks Akt phosphorylation and activation by an allosteric mechanism (DeFeo-Jones et al., 2005). Phosphorylation of Akt was abolished with 1 µM Akt inhibitor VIII (supplementary Fig. S2A). Akt inhibitor VIII sensitized LNT-229 cells towards CD95L- as well as towards TRAIL-mediated apoptosis (supplementary Fig. S2B, C).

Rapamycin is currently investigated in combination with several chemotherapeutics, including vincristine, VP-16, cisplatin and others for various malignancies (Haritunians et al., 2007). To test whether rapamycin might enhance the cytotoxicity of chemotherapeutic drugs administered for the treatment of patients with malignant glioma, we co-incubated LNT-229 cells with rapamycin and CCNU or vincristine (Fig. 2B). The cytotoxic effects of these drugs were not altered by co-incubation with rapamycin. It has recently been reported that rapamycin can cause activation of Akt and p42/44 MAPK through relieving feedback inhibitory mechanisms. To further address this issue, we performed immunoblot experiments with LNT-229 and U87MG cells after up to 24 h of exposure to rapamycin. However, rapamycin did not enhance Akt phosphorylation (Ser473) at any timepoint (supplementary Fig. S3A, B and Fig. 4A, lanes 2, 3). Stably transfected mTORsh cells also have unaltered P-Akt levels (Fig. 5D, lanes 1-4). Therefore, the feedback inhibition of Akt that has been found in the PTEN wild type prostate cancer cell line DU-145 and the breast cancer cell line MCF-7 (O'Reilly et al., 2006) is not present in LNT-229 or U87MG glioblastoma cells. We also failed to detect an increase in p42/44 MAPK phosphorylation in cells

exposed to rapamycin (supplementary Fig. S3A, B and Fig. 4A, lanes 2,3) and mTORsh cells (Fig. 5D, lanes 1-4) in contrast to the findings reported in other tumor types exposed to mTOR inhibitors (Carracedo et al., 2008).

Rapamycin causes growth inhibition in human malignant glioma cells but is not cytotoxic

Rapamycin exerts antiproliferative effects in a variety of human tumour cell lines (Easton and Houghton, 2006). Cytotoxic effects have also been reported in the human malignant glioma cell lines U87MG, T98G and U373MG (Takeuchi et al., 2005). To differentiate growth inhibitory from cytotoxic effects of rapamycin, cell growth and viability were assessed in parallel by crystal violet staining and flow cytometry for PI uptake in cells exposed to rapamycin or vehicle. In growth curves established in the presence of rapamycin, cell growth was decreased both in serum-free medium and medium containing 10% FCS in the cell lines LNT-229 and U87MG (Fig. 3A, B, left side). In the SV40-transformed astrocytic cell line SV-FHAS, the growth inhibitory effect of rapamycin was also potent with a cell growth of less than 50% in relation to the vehicle control in medium containing 10% FCS (data not shown). Cell viability was unaffected by exposure to rapamycin for up to 72 h (Fig. 3A, B, right side). Similar results were obtained in PTEN mutant T98G human malignant glioma cells and in long-term cultures with regular administration of rapamycin for several weeks (data not shown). PTEN wildtype LNT-229 and PTEN mutant U87MG and T98G cells showed similar sensitivity to rapamycin-induced growth inhibition without detection of rapamycin cytotoxicity. Also, similar growth inhibitory effects of rapamycin in the absence of cytotoxicity were observed in all primary cultures of human malignant gliomas investigated (Fig. 3C, supplementary Fig. S4A). Since the concomitant PI-staining did not reveal changes in the number of dead cells, the

observed effects are likely due to changes in proliferation. This is also corroborated by reduced [methyl-^{3}H]thymidine incorporation in 4 investigated primary glioblastoma cultures (supplementary Fig. S4B).

Hypoxia inhibits mTOR signalling and inhibition of mTOR signalling by rapamycin protects human malignant glioma cells from hypoxia-induced cell death

Hypoxia suppresses mTOR activity via the proteins REDD and TSC1/TSC2 (Brugarolas et al., 2004). This mechanism is considered an adaptive response allowing cells to survive under hypoxic and nutrient-deprived conditions by decreasing mTOR-dependent metabolic demands. To explore hypoxia-induced alterations of mTOR signalling, we employed a paradigm of hypoxia with partial glucose depletion and a defined mechanism of energy-dependent cell death of mainly necrotic features (Steinbach et al., 2004; Steinbach et al., 2003). The activity of mTOR targets was analysed by phospho-specific immunoblots. Under normoxic conditions, glucose restriction and serum withdrawal decreased the phosphorylation of Akt, RPS6 and S6K1 and shifted the pattern of the 4E-BP1 isoforms towards the lower hypophosphorylated α and β bands in LNT-229 cells (Fig. 4A). Rapamycin further suppressed S6K1 phosphorylation. Hypoxia had dramatic effects on mTOR signalling, abolishing phosphorylation of RPS6 and S6K1 and shifting 4E-BP1 phosphorylation utmost towards the lowest α band. Hypoxia also decreased the phosphorylation of p42/44 MAPK and this effect was enhanced by PD153035 (Fig. 4A). We had previously hypothesized that the protection from hypoxia conferred by inhibition of EGFR signalling is mediated by decreased mTOR activity (Steinbach et al., 2004). We therefore exposed LNT-229 cells to hypoxia in the presence of rapamycin or PD153035. Hypoxia-induced cell death was indeed reduced by

rapamycin (Fig. 4B). However, rapamycin was less potent than PD153035, indicating that PD153035 might exert its hypoxia-protective functions only partially via mTOR. Note that while PD153035 was cytotoxic under normoxic conditions, rapamycin was not (Fig. 4B, left graph). The hypoxia-protective effect of rapamycin became apparent at concentrations as low as 1 nM, with largely similar effects of concentration of 10 to 1000 nM in LNT-229 cells (supplementary Fig. S5A). Thus, low concentrations of rapamycin that are achieved in glioblastoma in vivo (Cloughesy et al., 2008) have the potential to protect glioblastoma cells from hypoxia while 1000-fold higher concentrations fail to induce cell death. The autophagy inhibitor 3-methyl-adenine did not abrogate PD153035 or rapamycin-mediated protection from hypoxia-induced cell death (data not shown). Also in ultrastructural analyses autophagy was not detectable in our model of hypoxia-induced cell death (Steinbach et al., 2005). Notably, rapamycin also protected cells derived from 2 out of 3 tested primary glioblastoma cultures from hypoxia-induced cell death, whereas PD153035 was effective in all (supplementary Fig. S5B). Furthermore, inhibition of Akt conferred protection from hypoxia (supplementary Fig. S2D); erlotinib also protected LNT-229 cells from hypoxia (supplementary Fig. S1B). Since mTOR exerts its effects in part via alterations of translation, the full impact of inhibition of mTOR may only become apparent when the levels of the target proteins have reached their (new) equilibrium. We therefore preincubated LNT-229 cells with rapamycin prior to exposure to hypoxia. Equal cell density in the differently preincubated cells was ensured by crystal violet staining prior to hypoxic conditioning and glucose restriction. Preincubation considerably enhanced the hypoxia-protective effect of rapamycin (Fig. 4C).

shRNA-mediated gene silencing of mTOR confers protection from hypoxia-induced cell death

Rapamycin exclusively inhibits the mTOR complex 1 (mTORC1), while the mTOR complex 2 (mTORC2), which contains mTOR in combination with different adaptor proteins, is resistant to rapamycin. To fully explore the role of the mTOR protein, we investigated the role of inhibition of mTOR using shRNA-mediated gene-silencing in stably transfected cells employing the pSUPER plasmid (Brummelkamp et al., 2002). The experiments were conducted with early-passage pooled clones. mTOR protein levels in LNT-229 cells stably transfected with the mTOR-directed sequence (LNT-229 mTORsh) were approximately 20% of those in LNT-229 cells transfected with the empty control vector (LNT-229 puro) (Fig. 5A). To investigate how gene suppression of mTOR impairs mTOR-mediated signal transduction, we stimulated serum-starved LNT-229 puro or mTORsh cells with EGF and IGF-1 to test for stimulated 4E-BP1 hyperphosphorylation (Brunn et al., 1997). After 24 h of incubation in serum-free medium, 4E-BP1 was detectable in both puro and mTORsh cells in the α and β bands evidencing a low phosphorylation state (Fig. 5B). In puro cells equal amounts of protein in the α and β bands were detectable, in mTORsh cells the extent of hypophosphorylation was more pronounced with more 4E-BP1 in the α than in the β band. 10 min incubation with EGF/IGF-1 led to an increase in phosphorylation of 4E-BP1 and a resulting band shift in both puro and mTORsh cells. Puro cells exhibited almost equal distributions of α, β and γ bands, whereas α and β bands were still dominating in mTORsh cells indicating a lesser degree of 4E-BP1 phosphorylation. Similar results were obtained with an antibody that detects total 4E-BP1. Thus, phosphorylation of the mTOR target 4E-BP1 is suppressed in mTORsh cells, confirming the functionality of the gene suppression. Rapamycin addition to the serum-starved cells 1 h prior to stimulation with EGF and IGF-1 abolished 4E-BP1

hyperphosphorylation as evidenced by the lacking γ band in cells incubated with EGF/IGF-1 (Fig. 5C). To test whether mTOR gene suppression has effects on EGFR-dependent signalling in our hypoxia model, we compared the phosphorylation patterns of p90RSK, p42/44 MAPK, Akt and RPS6 using total eIF4E as a loading control (Fig. 5D). In contrast to LNT-229 puro cells, RPS6 phosphorylation was already abolished in mTORsh cells after 8 h incubation in serum-free medium containing 2 mM glucose under normoxia (Fig. 5D, lanes 3, 4), again indicating an impaired mTOR activity in mTORsh cells. In contrast, equal amounts of P-RPS6 were detectable in cells incubated in medium containing 10% FCS (Fig. 5D, lanes 1, 2). Thus, with supra-physiological stimulation of starvation-sensitive pathways, the residual mTOR activity in the mTORsh cells is sufficient to maintain RPS6 phosphorylation. The phosphorylation patterns of the other investigated proteins not downstream of mTOR were comparable to those observed in LNT-229 wildtype cells (Fig. 4A). Of note, after 24 h incubation in serum-free medium without glucose deprivation LNT-229 mTORsh cells also exhibited a weaker RPS6 phosphorylation than puro control cells (data not shown). To test whether gene suppression of mTOR modulates the sensitivity to the chemotherapeutics CCNU or vincristine, we exposed LNT-229 puro or mTORsh cells to these drugs (Fig. 5E). Stable mTOR-knockdown cells were less sensitive to chemotherapy-induced cell death than puro control cells and rapamycin-treated cells. This effect may be explained either by long-term alterations of protein expression in the mTORsh cells or by a mTORC2-mediated mechanism.

To characterize the effect of gene suppression of mTOR on proliferation, growth curves in serum-free medium and medium containing 10% FCS were established in LNT-229 mTORsh and puro cells in the absence or presence of rapamycin. Gene suppression of mTOR reduced proliferation to a similar degree as rapamycin (Fig.

5F). Rapamycin further decreased the proliferation of LNT-229 mTORsh cells. Similar effects were observed with medium containing 10% FCS (Fig. 5F, bottom panel). The additive growth-inhibitory effect may be due to inhibition of the residual mTOR protein in the mTORsh cells. Alternatively, suppression of the mTORC2 function in the LNT-229 mTORsh cells may add to the effect of rapamycin.

We then compared the sensitivity to hypoxia of LNT-229 mTORsh and puro cells. LNT-229 mTORsh cells were resistant to hypoxia-induced cell death (Fig. 5G). The protection conferred by inhibition of EGFR signalling with PD153035 was more pronounced than that of gene suppression of mTOR. In addition, PD153035, in contrast to rapamycin, enhanced the protection from hypoxia observed in mTORsh cells. Therefore, mTOR-independent signalling cascades downstream of the EGFR appear to contribute to the protective effect of PD153035. Protection from hypoxia-induced cell death in LNT-229 mTORsh in comparison to LNT-229 puro cells was also detectable at the level of flow cytometric assessment of PI staining (data not shown).

Antagonism of mTOR signalling preserves cellular ATP and mitochondrial integrity

We have previously demonstrated that EGFR inhibition reduces glucose consumption, delays ATP depletion and preserves mitochondrial integrity during hypoxia (Steinbach et al., 2004). Similarly, in LNT-229 mTORsh cells as well as in rapamycin-pretreated LNT-229 cells, the hypoxia-induced depletion of ATP was delayed (Fig. 6A, B). Further, the percentage of cells with intact mitochondrial membrane potential after 16 h of hypoxic incubation was higher in LNT-229 mTORsh than in LNT-229 puro cells (Fig. 6C). Rapamycin preincubation, unlike EGFR inhibition, did not alter glucose consumption under hypoxic conditions (data not shown) in accordance with a previous report that rapamycin does not alter glucose

consumption in LN-229 cells under normoxia (Wei et al., 2008). Glucose consumption was also unchanged in LNT-229 mTORsh cells compared with LNT-229 puro cells (Fig. 6D). These results indicate that antagonizing mTOR reduces energy demand, thus preserving cellular viability independent from glucose consumption.

HIF-1 α is considered one mediator of mTOR-induced adaptive responses to hypoxia and HIF-1 α protein levels have been reported to decrease in response to mTOR inhibition with the rapamycin analogue CCI-779 in kidney cancer cells (Thomas et al., 2006). Independent from its effects in angiogenesis, HIF-1 α adapts metabolic processes by altering the transcription of a large number of target genes (Semenza et al., 1994). Therefore we investigated HIF-1 α protein by immunoblot analysis in LNT-229 cells exposed to rapamycin or PD153035, both under normoxic and hypoxic conditions (Fig. 6E). Neither rapamycin nor PD153035 altered the induction of HIF-1 α by hypoxia. HIF-1 α levels were also maintained in hypoxic LNT-229 mTORsh cells (Fig. 6F).

Cycling cells are more sensitive to induction of apoptosis and have higher energy consumption. We therefore investigated the expression of the cell cycle regulator cyclin D1, another protein which that has been reported to be regulated in a mTOR-dependent fashion (Averous et al., 2008). Rapamycin did not alter cyclin D1 protein levels (Fig. 6G). Thus, malignant glioma cells maintain the expression of molecules critical for proliferation, angiogenesis and metabolic adaptive function independently from mTOR.

Discussion:

In an attempt to dissociate pathways responsible for two opposing major effects of EGFR signalling, we have explored to what extent mTOR mediates proapoptotic effects and metabolic hypoxia-protective effects of EGFR inhibition.

We find that rapamycin is not cytotoxic to human malignant glioma cells as assessed by LDH release or PI assays. Of note, neither the viability of permanent cell lines nor that of primary cultures derived from glioma surgical specimens was affected by rapamycin (Fig. 3A-C, supplementary Fig. S4A). Further, whereas EGFR or Akt inhibition sensitized malignant glioma cells to the death ligand CD95L or TRAIL, rapamycin failed to sensitize these cells to CD95L, TRAIL or chemotherapeutic drugs such as CCNU or vincristine (Fig. 2A, B, supplementary Fig. S1A, S2B, C). Notably, the failure of rapamycin was not due to feedback activation of Akt or p42/44 MAPK which has been described in other tumour types (Carracedo et al., 2008; O'Reilly et al., 2006) (supplementary Fig. S3A, B). Therefore, dissociation of proapoptotic effects at the level of Akt remains the most plausible explanation for the absence of cytotoxicity of mTOR antagonistic strategies.

These findings are corroborated by similar results observed in response to mTOR gene suppression (Fig. 5E, F). Stable mTOR-knockdown cells were even less sensitive to chemotherapy-induced cell death than puro control cells. This observation is in accordance with a recent report from Lee et al. who report that antagonism of mTOR in TSC-deficient fibroblasts protects these cells against DNA-damage and etoposide by reducing p53-dependent cell death (Lee et al., 2007). Importantly, mTOR inhibition also did not induce synergistic effects when combined with inhibitors of EGFR, PI3K or MAPK, respectively (Fig. 2A). Since pilot trials investigating combinations of inhibitors of EGFR and mTOR are underway (Doherty et al., 2006; Reardon et al., 2006), this is of particular concern.

The widely held assumption that downstream effects of PI3K and Akt are necessarily mediated by mTOR is also challenged by the findings of Opel et al. who found that Akt activation is associated with decreased event-free or overall survival in neuroblastoma patients whereas phosphorylation of the prototypical mTOR target RPS6 is not (Opel et al., 2007). The same authors have recently reported that inhibition of mTOR fails to sensitize both PTEN wildtype and PTEN mutant human malignant glioma cells from established cell lines as well as from primary cultured glioblastoma samples towards cell death induced by TRAIL or chemotherapy, in line with our findings (Opel et al., 2008). Thus, at least for glioma cells, the current view of mTOR as an apoptosis-modulating target of Akt needs to be reconsidered.

It is intriguing to speculate that the observed dissociation of hypoxia-protective effects and antiapoptotic effects on the level of mTOR could be due to effects of EGFR inhibition that are not mediated by impaired EGFR kinase function as recently described (Weihua et al., 2008). However, it is notable that the effects described by Weihua et al. were only observed with gene suppression, which reduces EGFR protein expression necessary for the function of the glucose transporter SGLT1, not with EGFR kinase inhibitors such as PD153035, which was employed in our study. The similar effects achieved with erlotinib support this conclusion (supplementary Fig. S1A and S1B).

Further, both types of consequences of EGFR inhibition – protection from hypoxia, as well as enhanced apoptosis – can be mimicked by inhibitors of EGFR-dependent signal transduction. Co-inhibition of PI3K and MEK, in contrast to co-inhibition of mTOR and MEK, sensitizes glioma cells towards CD95L (see Fig. 2A and supplementary Fig. S1C). Protection from hypoxia-induced cell death in cells co-exposed to LY294002 and U0126 has previously been demonstrated (Steinbach et al., 2004).

The experiments with the Akt-specific inhibitor Akt inhibitor VIII further clarify the level of EGFR-dependent signal transduction that mediates the proapoptotic consequences (supplementary Fig. S2B, C)(DeFeo-Jones et al., 2005). Since inhibition of Akt also conferred protection from hypoxia (supplementary Fig. S2D), our data are well compatible with a dissociation of pro-apoptotic and hypoxia-protective effects downstream of Akt. A recent report implicates protein kinase C (PKC) as the mediator of EGFR signalling to mTOR independently of Akt, dissecting mTOR from the Akt-signalling cascade and challenging the widely held assumption of mTOR as a downstream target of Akt (Fan et al., 2009). In our experimental setting, however, Akt inhibition mimicked both the pro-apoptotic and the hypoxia-protective effects of EGFR inhibition whereas mTOR inhibition only mimicked the hypoxia-protective effects. Whether parallel rather than serial signal pathways are more relevant for regulation of mTOR by EGFR through Akt, PKC or both thus remains to be determined. We have incorporated our data and this new finding in a schematic drawing summarizing the proposed functions of signalling molecules in glioblastoma cells (supplementary Fig. S6).

Deleted: also

Deleted: these

Even more striking than its lack of toxicity, mTOR antagonism exerts powerful cytoprotective effects on hypoxic glioma cells (Fig. 4B, C; Fig. 5G). mTOR is a master regulator of cellular energy homeostasis and, under physiologic conditions, reduced mTOR activity as a consequence of impaired nutrient availability enables cells to survive by adapting metabolic processes (Lee et al., 2007; Peng et al., 2002). Therefore, the hypoxia-protective effects of mTOR inhibition should not come entirely unexpected. Our results suggest that, in patients with malignant glioma, mTOR inhibition may jeopardize the antitumour effects of both spontaneously occurring tumour hypoxia and hypoxia resulting from antiangiogenic therapies and may contribute to adverse outcome. This hypothesis is based on studies demonstrating

that sublethal hypoxia is a major selective pressure driving and maintaining genetic instability and a mutator phenotype which leads to the selection of more aggressive tumour cell clones (Bristow and Hill, 2008) exhibiting therapy-resistance with reduced apoptotic potential (Graeber et al., 1996) and increased invasive properties (Pennacchietti et al., 2003). Hypoxia-protective effects of rapamycin have also been observed in mouse LLC cells (Hamanaka et al., 2005). The protection from hypoxia conferred by mTOR antagonism in conjunction with its lack of cytotoxicity may offer an explanation for the disappointing results of clinical trials with mTOR inhibitors for recurrent glioblastoma (Galanis et al., 2005). It may be prudent to consider undesirable effects originating from alterations of cellular metabolism and energy homeostasis for strategies targeting the EGFR-PI3K-Akt axis at any molecule, upstream (Steinbach et al., 2004) or downstream of mTOR. The validity of the assumption that the protection from hypoxia conferred by the inhibition of EGFR and mTOR could result in clinically relevant adverse effects is supported by recent data from clinical trials combining EGFR inhibition with antiangiogenetic agents. Lassen et al. (ASCO annual meeting 2008, abstract #2056) presented data from a trial with erlotinib in combination with bevacizumab and irinotecan in patients with progressive glioblastoma. Progression-free survival at 6 months in this one-armed trial was at a disappointing level of 24%, as compared with 48% in the original study with bevacizumab and irinotecan (Wagner et al., ASCO annual meeting 2008, abstract #2021). Overt antagonistic effects of the anti-EGFR antibody cetuximab were demonstrated in a randomized phase III trial comparing bevacizumab plus chemotherapy alone or combined with cetuximab in patients with colon cancer (Tol et al., 2008). Notably, the hypoxia-protective effect of EGFR inhibition *in vitro* is also detectable in colon carcinoma cells (S. Wolking, J. Rieger and J. P. Steinbach, unpublished data).

The complexity of the metabolic response of human malignant glioma cells towards hypoxia is further illustrated by the dissociation of mTOR signalling and HIF-1 α. In non-transformed cells and some tumour cell lines, mTOR induces HIF-1 α expression, possibly via a posttranslational mechanism (Hudson et al., 2002). Given that hypoxia suppresses mTOR signalling in malignant glioma cells (Fig. 4A), this mechanism should result in reduced expression of HIF-1 α. However, levels of HIF-1 α protein were maintained in hypoxic mTORsh cells and cells exposed towards rapamycin (Fig. 6E, F). One plausible explanation is that hypoxic glioma cells are under selective pressure to maintain HIF-1 α-dependent neoangiogenesis. Since HIF-1 α also exerts metabolic effects important for the adaptation of tumour cells to hypoxic conditions (Brahimi-Horn and Pouyssegur, 2007), the capability of glioma cells to maintain HIF-1 α expression independently of mTOR may also be important for the rapamycin-induced protection from hypoxic cell death. HIF-1 α -antagonistic strategies therefore, potentially, could revert mTOR inhibition-dependent resistance towards hypoxia. Finally, mTOR inhibition may have valuable anti-tumour effects that only become apparent *in vivo*. First, it has been shown that rapamycin specifically sensitizes U87MG cell xenografts towards radiotherapy while single layer cultures are not affected (Eshleman et al., 2002). Notably, in that study rapamycin failed to demonstrate in vivo growth-inhibitory effects in spite of the known antiproliferative effects in vitro and the probable antiangiogenic effects, again suggesting mechanisms of rapamycin resistance such as decreased susceptibility towards hypoxia. Further, rapamycin also has antiangiogenic properties, some of which may be dependent on HIF-1 α (Del Bufalo et al., 2006; Phung et al., 2007), whereas others may be dependent on direct cytotoxic effects of rapamycin on human endothelial cells (Barilli et al., 2008). These properties, in conjunction with the strong antiproliferative effects of rapamycin and its low toxicity as well as the successful

clinical trials of mTOR-inhibition for other tumour types, e.g., renal cell carcinoma, warrant further studies of mTOR inhibition in malignant glioma patients.

A recently reported neoadjuvant trial of rapamycin treatment prior to scheduled resection of recurrent glioblastoma with PTEN loss followed by rapamycin maintenance therapy demonstrated that nanomolar concentrations of rapamycin can be achieved in glioblastoma (Cloughesy et al., 2008). The authors concluded that rapamycin reduced proliferation in patients with evidence of decreased RPS6 phosphorylation. The median time to progression with adjuvant rapamycin therapy after surgery was only 99 days in this molecular enriched population, although there was some evidence of clinical activity. These results are well compatible with our finding of growth inhibition as the principal anti-tumour effect of rapamycin and suggest mechanisms of resistance towards rapamycin other than insufficient tumour penetration.

Inhibition of mTOR may be most successful in the setting of primary therapy in combination with radiotherapy. The risk for a clinically relevant negative impact of the hypoxia-protective effects of mTOR inhibition would plausibly be lowest for patients who have undergone macroscopically complete resections of their tumours that should minimize the occurrence of hypoxia. These issues will be addressed in a forthcoming clinical study with the non-immunosuppressant mTOR Inhibitor CCI-779 in combination with radiotherapy versus radiotherapy alone in the primary therapy of glioblastoma with unmethylated MGMT-promoter that will be conducted by the EORTC brain tumour group (W. Wick, personal information).

Funding:

This work was supported by the Medical Faculty, Interdisciplinary Clinical Research Center (IZKF), of the University of Tübingen.

Introduction + materials and methods + results + discussion + funding: 6574 words

Figure legends

Fig. 1. *Concentration-dependent inhibition of S6K1 phosphorylation by rapamycin in human malignant glioma cells.*

LNT-229 or U87MG cells were exposed to vehicle or rapamycin (0.1-1000 nM) in serum-free medium for 20 min. Levels of phosphorylated and total S6K1 protein were analysed by immunoblot.

Fig. 2. *Effects of pharmacological manipulation of EGFR-Akt-mTOR signalling on CD95L- and chemotherapy-induced cell death.*

A, upper panel. LNT-229 or U87MG cells were exposed to vehicle, rapamycin (100 nM), PD153035 (10 µM), LY294002 (10 µM) or U0126 (20 µM) alone or combined as indicated in serum-free medium for 20 min for immunoblot analysis. Cellular lysates were analysed for P-p90^{RSK}, P-Akt, P-p42/44 MAPK, P-RPS6, eIF4E, P-4E-BP1 or 4E-BP1. Lower panel. LNT-229 cells were exposed to 100 U/ml CD95L, U87MG cells were exposed to 20 U/ml CD95L for 24 h. Cell density was assessed by crystal violet staining, cell densities are normalised and shown as percentages of the cell densities when inhibitors were used as single agents or combinations without CD95L (n=3, * $P < 0.05$ corrected for multiple testing, student's *t*-test).

B, LNT-229 cells were co-incubated with vehicle or 100 nM rapamycin and exposed to CCNU or vincristine for 72 h. Cell density was assessed by crystal violet staining (n=3, all *P-values* were > 0.05, student's *t*-test).

Fig. 3. *Effects of rapamycin on viability and proliferation.*

A, **B**, **C**, To assess proliferation, LNT-229 (A), or U87MG (B) cells and primary glioblastoma cultures (C) were exposed to vehicle or 100 nM rapamycin in serum-

free medium or medium containing 10% FCS. Cell density was assessed by crystal violet staining (n≥3, * $P < 0.05$, ** $P < 0.01$, student's *t*-test). The cell growth of vehicle-treated cells after 72 h corresponds to 100%. For viability analysis, cells were incubated in serum-free medium with rapamycin for 72 h. PI uptake was quantified by flow cytometry. The spontaneously occurring percentage of PI-positive cells was not enhanced by rapamycin.

Fig. 4. *Effects of rapamycin on hypoxia-induced cell death and hypoxia-induced alterations of mTOR signalling.*

A, LNT-229 cells were cultured in medium containing 10% FCS or in serum-free medium containing 2 mM glucose and exposed to vehicle, 100 nM rapamycin or 10 µM PD153035 under normoxia or hypoxia for 8 h as indicated. Cellular lysates were analysed with antibodies to P-p90^{RSK}, P-Akt, P-p42/44 MAPK, P-RPS6, eIF4E, P-S6K1, S6K1, P-4E-BP1, 4E-BP1 or actin.

B, LNT-229 cells were incubated in serum-free medium containing 2 mM glucose and exposed to vehicle, 100 nM rapamycin or 10 µM PD153035 under normoxia or hypoxia for 20 h. Cytotoxicity was assessed by LDH release (n=4, n.s. $P > 0.05$, ** $P < 0.01$, student's *t*-test).

C, LNT-229 cells were pre-incubated for 24 h in serum-free medium with either vehicle or 100 nM rapamycin, followed by exposure to normoxia or hypoxia in serum-free medium containing 2 mM glucose in the presence of rapamycin or vehicle for 20 h. Hypoxia-induced cell death was assessed by LDH release (n=4, ** $P < 0.01$, student´s *t*-test). Note that the slightly higher amount of hypoxia-induced cell death in untreated cells compared to B is due to a higher cell growth.

Fig. 5. *shRNA-mediated gene silencing of mTOR: effects on chemotherapy-induced cell death, proliferation and hypoxia-induced cell death.*

A, LNT-299 cells were transfected with either the empty pSUPER puro vector (puro) or the pSUPER puro plasmid with the mTOR-directed small hairpin sequence (mTORsh). Cellular lysates were analysed by immunoblot with antibodies to mTOR and actin.

B, LNT-229 puro or mTORsh cells were incubated in serum-free medium for 24 h and subsequently exposed to serum-free medium containing 100 ng/ml EGF and 50 ng/ml IGF-1 for 10 min. Cellular lysates were analysed by immunoblot with antibodies to P-4E-BP1, 4E-BP1 or actin.

C, LNT-229 puro or mTORsh cells were incubated in serum-free medium for 23 h, then rapamycin was added to a final concentration of 100 nM. After 1 h cells were exposed to serum-free medium containing 100 ng/ml EGF and 50 ng/ml IGF-1 and 100 nM rapamycin for 20 min. Cellular lysates were analysed by immunoblot with antibodies to P-4E-BP1 or actin.

D, LNT-229 puro and mTORsh cells were incubated in medium containing 10% FCS or in serum-free medium containing 2 mM glucose under normoxia (N8) or hypoxia (H8) for 8 h as indicated. Cellular lysates were analysed with antibodies to P-p90^{RSK}, P-Akt, P-p42/44 MAPK, P-RPS6 and eIF4E.

E, LNT-229 puro and mTORsh cells were exposed to CCNU or vincristine in serum-free medium for 72 h. Cell density was assessed by crystal violet staining (n=3, * $P < 0.05$, ** $P < 0.01$, student's *t*-test).

F, LNT-229 puro and mTORsh cells were incubated in serum-free medium or medium containing 10% FCS and exposed to vehicle or 100 nM rapamycin for the indicated periods of time. Cell density was assessed by crystal violet staining (n=3, n.s. $P > 0.05$, * $P < 0.05$, ** $P < 0.01$, student's *t*-test).

G, LNT-229 puro and mTORsh cells were incubated in serum-free medium containing 2 mM glucose and exposed to vehicle, 100 nM rapamycin or 10 µM PD153035 in hypoxia for 20 h. Cytotoxicity was assessed by LDH release (n=4, * $P < 0.05$, ** $P < 0.01$, student's *t*-test).

Fig. 6. *Effects of rapamycin and mTOR gene suppression on energy homeostasis.*

A, LNT-229 puro or mTORsh cells were incubated in serum-free medium containing 2 mM glucose and exposed to vehicle or 10 µM PD153035 under normoxia or hypoxia for 12 h. Cellular ATP (percent of normoxic controls) was determined by luciferase assay (n=4, ** $P < 0.01$, student's *t*-test).

B, LNT-229 cells were preincubated in serum-free medium with vehicle or 100 nM rapamycin for 24 h. Subsequently the cells were incubated in serum-free medium containing 2 mM glucose and exposed to vehicle or 100 nM rapamycin under normoxia or hypoxia for 12 h. Cellular ATP was determined by luciferase assay (n=3, * $P < 0.05$, student's *t*-test).

C, LNT-229 puro and mTORsh cells were incubated in serum-free medium containing 2 mM glucose under normoxia or hypoxia for 16 h. Mitochondrial membrane potential was determined by JC-1 staining and analysed by flow cytometry.

D, LNT-229 puro or mTORsh cells were incubated in serum-free medium containing 2 mM glucose under hypoxia for 4 h. Glucose concentration in the supernatant was determined enzymatically (n=4, n.s. $P > 0.05$, student's *t*-test).

E, LNT-229 cells were incubated in medium containing 10% FCS or in serum-free medium containing 2 mM glucose and exposed to vehicle, 100 nM rapamycin or 10 µM PD153035 under normoxia or hypoxia for 8 h. Cellular lysates were analysed by immunoblot with antibodies to HIF-1 α or actin.

F, LNT-229 puro or mTORsh cells were incubated in serum-free medium containing 2 mM glucose under normoxia or hypoxia for 8 h. Cellular lysates were analysed by immunoblot with antibodies to HIF-1 α or actin.

G, LNT-229 cells were incubated in medium containing 10% FCS or serum-free medium and exposed to vehicle or 100 nM rapamycin for 24 h. Cellular lysates were analysed by immunoblot with antibodies to cyclin D1 or actin.

Figure legends - supplementary figures

Fig. S1. *Effects of erlotinib and reduced concentrations of LY294002 and U0126 on CD95L-induced cell death and effect of erlotinib on hypoxia-induced cell death.*

A, LNT-229 cells were exposed to vehicle or 10 µM erlotinib in the presence of vehicle or 100 U/ml CD95L for 24 h. Cell density was assessed by crystal violet staining, normalised and shown as percentages of the cell densities when vehicle or erlotinib were used as single agents without CD95L (n=3, ** $P < 0.01$, student's *t*-test).

B, LNT-229 cells were incubated in serum-free medium containing 2 mM glucose and exposed to vehicle or 10 µM erlotinib under hypoxia (1% oxygen) for 72 h. Cytotoxicity was assessed by PI staining (n=2, * $P < 0.05$, student's *t*-test).

C, LNT-229 cells were exposed to vehicle, 5 µM LY294002, or 10 µM U0126 or both in the presence of vehicle or 100 U/ml CD95L for 20 h. Cell density was assessed by crystal violet staining, normalised and shown as percentages of the cell densities when vehicle or inhibitors were used as single agents without CD95L (n=3, * $P < 0.05$ corrected for multiple testing, student's *t*-test).

Fig. S2. *Effects of inhibition of Akt signalling on CD95L-, TRAIL- and hypoxia-induced cell death.*

A, LNT-229 cells were exposed to vehicle or Akt inhibitor VIII (0.1-10 µM) in serum-free medium for 30 min. Levels of phosphorylated and total Akt protein were analysed by immunoblot.

B, **C**, LNT-229 cells were exposed to vehicle, 100 nm rapamycin or 1 µM Akt inhibitor VIII in the presence of vehicle or 100 U/ml CD95L (A) or 1000 ng/ml TRAIL (B) for 24 h. Cell density was assessed by crystal violet staining, normalised and shown as percentages of the cell densities when inhibitors were used as single agents without CD95L or TRAIL (n=3, ** $P < 0.01$, student's *t*-test).

D, LNT-229 cells were incubated in serum-free medium containing 2 mM glucose and exposed to vehicle or 1 µM Akt inhibitor VIII under hypoxia for 20 h. Cytotoxicity was assessed by PI staining, representative results of one of four reproductions are shown.

Fig. S3. *Effects of rapamycin on p42/44 MAPK and Akt phosphorylation.*

A, **B**, LNT-229 (A) and U87MG (B) cells were incubated in serum-free medium containing vehicle or 100 nM rapamycin for 1, 3, 6, 12 or 24 h. Cellular lysates were analysed with antibodies to P-Akt, Akt, P-p42/44 MAPK, p42/44 MAPK, P-RPS6, eIF4E and actin.

Fig. S4. *Effects of rapamycin on viability and proliferation of primary glioblastoma cultures.*

A, To assess proliferation primary glioblastoma cultures were exposed to vehicle or 100 nM rapamycin in serum-free medium or medium containing 10% FCS. Cell density was assessed by crystal violet staining ($n \geq 3$, * $P < 0.05$, ** $P < 0.01$,

student's *t*-test). The cell growth of vehicle-treated cells after 72 h corresponds to 100%. For viability analysis, cells were incubated in serum-free medium with rapamycin for 72 h. PI uptake was quantified by flow cytometry. The spontaneously occurring percentage of PI-positive cells was not enhanced by rapamycin.

B, To further assess proliferation, primary glioblastoma cultures were exposed to vehicle or 100 nM rapamycin in serum-free medium or medium containing 10% FCS for 48 h, then cells were pulsed with 1 µCi [methyl-^{3}H]thymidine for additional 16 h. [Methyl-^{3}H]thymidine incorporation was assessed by a liquid scintillation counter ($n \geq 3$, * $P < 0.05$, ** $P < 0.01$, student's *t*-test).

Fig. S5. *Effects of rapamycin on hypoxia-induced cell death.*

A, LNT-229 cells were incubated in serum-free medium containing 2 mM glucose and exposed to vehicle, 1, 10, 100, 1000 nM rapamycin or 10 µM PD153035 under hypoxia for 20 h. Cytotoxicity was assessed by LDH release ($n = 4$, * $P < 0.05$, ** $P < 0.01$, student's *t*-test).

B, Primary glioblastoma cultures were incubated in serum-free medium containing 2 mM glucose and exposed to vehicle, 100 nM rapamycin or 10 µM PD153035 under hypoxia for 20 h. Cytotoxicity was assessed by LDH release ($n = 4$, * $P < 0.05$, ** $P < 0.01$, student's *t*-test).

Fig. S6. *Schematic drawing summarizing the proposed functions of signalling molecules in glioblastoma cells.*

References

Averous J, Fonseca BD, Proud CG. Regulation of cyclin D1 expression by mTORC1 signaling requires eukaryotic initiation factor 4E-binding protein 1. Oncogene 2008; 27: 1106-13.

Bahr O, Rieger J, Duffner F, Meyermann R, Weller M, Wick W. P-glycoprotein and multidrug resistance-associated protein mediate specific patterns of multidrug resistance in malignant glioma cell lines, but not in primary glioma cells. Brain Pathol 2003; 13: 482-94.

Barilli A, Visigalli R, Sala R, Gazzola GC, Parolari A, Tremoli E, et al. In human endothelial cells rapamycin causes mTORC2 inhibition and impairs cell viability and function. Cardiovasc Res 2008.

Brahimi-Horn MC, Pouyssegur J. Hypoxia in cancer cell metabolism and pH regulation. Essays Biochem 2007; 43: 165-78.

Bristow RG, Hill RP. Hypoxia and metabolism. Hypoxia, DNA repair and genetic instability. Nat Rev Cancer 2008; 8: 180-92.

Brugarolas J, Lei K, Hurley RL, Manning BD, Reiling JH, Hafen E, et al. Regulation of mTOR function in response to hypoxia by REDD1 and the TSC1/TSC2 tumor suppressor complex. Genes Dev 2004; 18: 2893-904.

Brummelkamp TR, Bernards R, Agami R. A system for stable expression of short interfering RNAs in mammalian cells. Science 2002; 296: 550-3.

Brunn GJ, Hudson CC, Sekulic A, Williams JM, Hosoi H, Houghton PJ, et al. Phosphorylation of the translational repressor PHAS-I by the mammalian target of rapamycin. Science 1997; 277: 99-101.

Carracedo A, Ma L, Teruya-Feldstein J, Rojo F, Salmena L, Alimonti A, et al. Inhibition of mTORC1 leads to MAPK pathway activation through a PI3K-dependent feedback loop in human cancer. J Clin Invest 2008; 118: 3065-74.

Choe G, Horvath S, Cloughesy TF, Crosby K, Seligson D, Palotie A, et al. Analysis of the phosphatidylinositol 3'-kinase signaling pathway in glioblastoma patients in vivo. Cancer Res 2003; 63: 2742-6.

Cloughesy TF, Yoshimoto K, Nghiemphu P, Brown K, Dang J, Zhu S, et al. Antitumor activity of rapamycin in a Phase I trial for patients with recurrent PTEN-deficient glioblastoma. PLoS Med 2008; 5: e8.

DeFeo-Jones D, Barnett SF, Fu S, Hancock PJ, Haskell KM, Leander KR, et al. Tumor cell sensitization to apoptotic stimuli by selective inhibition of specific Akt/PKB family members. Mol Cancer Ther 2005; 4: 271-9.

Del Bufalo D, Ciuffreda L, Trisciuoglio D, Desideri M, Cognetti F, Zupi G, et al. Antiangiogenic potential of the Mammalian target of rapamycin inhibitor temsirolimus. Cancer Res 2006; 66: 5549-54.

Doherty L, Gigas DC, Kesari S, Drappatz J, Kim R, Zimmerman J, et al. Pilot study of the combination of EGFR and mTOR inhibitors in recurrent malignant gliomas. Neurology 2006; 67: 156-8.

Easton JB, Houghton PJ. mTOR and cancer therapy. Oncogene 2006; 25: 6436-46.

Eshleman JS, Carlson BL, Mladek AC, Kastner BD, Shide KL, Sarkaria JN. Inhibition of the mammalian target of rapamycin sensitizes U87 xenografts to fractionated radiation therapy. Cancer Res 2002; 62: 7291-7.

Fan QW, Cheng C, Knight ZA, Haas-Kogan D, Stokoe D, James CD, et al. EGFR signals to mTOR through PKC and independently of Akt in glioma. Sci Signal 2009; 2: ra4.

Galanis E, Buckner JC, Maurer MJ, Kreisberg JI, Ballman K, Boni J, et al. Phase II trial of temsirolimus (CCI-779) in recurrent glioblastoma multiforme: a North Central Cancer Treatment Group Study. J Clin Oncol 2005; 23: 5294-304.

Gingras AC, Raught B, Gygi SP, Niedzwiecka A, Miron M, Burley SK, et al. Hierarchical phosphorylation of the translation inhibitor 4E-BP1. Genes Dev 2001; 15: 2852-64.

Graeber TG, Osmanian C, Jacks T, Housman DE, Koch CJ, Lowe SW, et al. Hypoxia-mediated selection of cells with diminished apoptotic potential in solid tumours. Nature 1996; 379: 88-91.

Haas-Kogan DA, Prados MD, Tihan T, Eberhard DA, Jelluma N, Arvold ND, et al. Epidermal growth factor receptor, protein kinase B/Akt, and glioma response to erlotinib. J Natl Cancer Inst 2005; 97: 880-7.

Hamanaka Y, Mukai M, Shimamura M, Kitagawa T, Nishida T, Isohashi F, et al. Suppression of PI3K/mTOR pathway rescues LLC cells from cell death induced by hypoxia. Biochem Biophys Res Commun 2005; 330: 318-26.

Hara K, Yonezawa K, Kozlowski MT, Sugimoto T, Andrabi K, Weng QP, et al. Regulation of eIF-4E BP1 phosphorylation by mTOR. J Biol Chem 1997; 272: 26457-63.

Haritunians T, Mori A, O'Kelly J, Luong QT, Giles FJ, Koeffler HP. Antiproliferative activity of RAD001 (everolimus) as a single agent and combined with other agents in mantle cell lymphoma. Leukemia 2007; 21: 333-9.

Harris TE, Lawrence JC, Jr. TOR signaling. Sci STKE 2003; 2003: re15.

Hay N, Sonenberg N. Upstream and downstream of mTOR. Genes Dev 2004; 18: 1926-45.

Hidalgo M, Rowinsky EK. The rapamycin-sensitive signal transduction pathway as a target for cancer therapy. Oncogene 2000; 19: 6680-6.

Huang S, Houghton PJ. Mechanisms of resistance to rapamycins. Drug Resist Updat 2001; 4: 378-91.

Hudson CC, Liu M, Chiang GG, Otterness DM, Loomis DC, Kaper F, et al. Regulation of hypoxia-inducible factor 1alpha expression and function by the mammalian target of rapamycin. Mol Cell Biol 2002; 22: 7004-14.

Ishii N, Maier D, Merlo A, Tada M, Sawamura Y, Diserens AC, et al. Frequent co-alterations of TP53, p16/CDKN2A, p14ARF, PTEN tumor suppressor genes in human glioma cell lines. Brain Pathol 1999; 9: 469-79.

Kleihues P, Burger PC, Collins VP, Newcomb EW, Ohgaki H, Cavenee WK. Glioblastoma. In: Kleihues P and Cavenee WK, editors. Pathology and Genetics of Tumours of the Nervous System. Lyon: IARC press, 2000: 29-39.

Lee CH, Inoki K, Karbowniczek M, Petroulakis E, Sonenberg N, Henske EP, et al. Constitutive mTOR activation in TSC mutants sensitizes cells to energy starvation and genomic damage via p53. Embo J 2007; 26: 4812-23.

Mendelsohn J. Targeting the epidermal growth factor receptor for cancer therapy. J Clin Oncol 2002; 20: 1S-13S.

Neshat MS, Mellinghoff IK, Tran C, Stiles B, Thomas G, Petersen R, et al. Enhanced sensitivity of PTEN-deficient tumors to inhibition of FRAP/mTOR. Proc Natl Acad Sci U S A 2001; 98: 10314-9.

Ohgaki H, Dessen P, Jourde B, Horstmann S, Nishikawa T, Di Patre PL, et al. Genetic pathways to glioblastoma: a population-based study. Cancer Res 2004; 64: 6892-9.

Opel D, Poremba C, Simon T, Debatin KM, Fulda S. Activation of Akt predicts poor outcome in neuroblastoma. Cancer Res 2007; 67: 735-45.

Opel D, Westhoff MA, Bender A, Braun V, Debatin KM, Fulda S. Phosphatidylinositol 3-kinase inhibition broadly sensitizes glioblastoma cells to death receptor- and drug-induced apoptosis. Cancer Res 2008; 68: 6271-80.

O'Reilly KE, Rojo F, She QB, Solit D, Mills GB, Smith D, et al. mTOR inhibition induces upstream receptor tyrosine kinase signaling and activates Akt. Cancer Res 2006; 66: 1500-8.

Pende M, Um SH, Mieulet V, Sticker M, Goss VL, Mestan J, et al. S6K1(-/-)/S6K2(-/-) mice exhibit perinatal lethality and rapamycin-sensitive 5'-terminal oligopyrimidine mRNA translation and reveal a mitogen-activated protein kinase-dependent S6 kinase pathway. Mol Cell Biol 2004; 24: 3112-24.

Peng T, Golub TR, Sabatini DM. The immunosuppressant rapamycin mimics a starvation-like signal distinct from amino acid and glucose deprivation. Mol Cell Biol 2002; 22: 5575-84.

Pennacchietti S, Michieli P, Galluzzo M, Mazzone M, Giordano S, Comoglio PM. Hypoxia promotes invasive growth by transcriptional activation of the met protooncogene. Cancer Cell 2003; 3: 347-61.

Phung TL, Eyiah-Mensah G, O'Donnell RK, Bieniek R, Shechter S, Walsh K, et al. Endothelial Akt signaling is rate-limiting for rapamycin inhibition of mouse mammary tumor progression. Cancer Res 2007; 67: 5070-5.

Rao RD, Mladek AC, Lamont JD, Goble JM, Erlichman C, James CD, et al. Disruption of parallel and converging signaling pathways contributes to the synergistic antitumor effects of simultaneous mTOR and EGFR inhibition in GBM cells. Neoplasia 2005; 7: 921-9.

Reardon DA, Quinn JA, Vredenburgh JJ, Gururangan S, Friedman AH, Desjardins A, et al. Phase 1 trial of gefitinib plus sirolimus in adults with recurrent malignant glioma. Clin Cancer Res 2006; 12: 860-8.

Reinhard C, Fernandez A, Lamb NJ, Thomas G. Nuclear localization of p85s6k: functional requirement for entry into S phase. Embo J 1994; 13: 1557-65.

Roth W, Fontana A, Trepel M, Reed JC, Dichgans J, Weller M. Immunochemotherapy of malignant glioma: synergistic activity of CD95 ligand and chemotherapeutics. Cancer Immunol Immunother 1997; 44: 55-63.

Roux PP, Shahbazian D, Vu H, Holz MK, Cohen MS, Taunton J, et al. RAS/ERK signaling promotes site-specific ribosomal protein S6 phosphorylation via RSK and stimulates cap-dependent translation. J Biol Chem 2007; 282: 14056-64.

Semenza GL, Roth PH, Fang HM, Wang GL. Transcriptional regulation of genes encoding glycolytic enzymes by hypoxia-inducible factor 1. J Biol Chem 1994; 269: 23757-63.

Steinbach JP, Klumpp A, Wolburg H, Weller M. Inhibition of epidermal growth factor receptor signaling protects human malignant glioma cells from hypoxia-induced cell death. Cancer Res 2004; 64: 1575-8.

Steinbach JP, Supra P, Huang HJ, Cavenee WK, Weller M. CD95-mediated apoptosis of human glioma cells: modulation by epidermal growth factor receptor activity. Brain Pathol 2002; 12: 12-20.

Steinbach JP, Weller M. Mechanisms of apoptosis in central nervous system tumors: application to theory. Curr Neurol Neurosci Rep 2002; 2: 246-53.

Steinbach JP, Wolburg H, Klumpp A, Probst H, Weller M. Hypoxia-induced cell death in human malignant glioma cells: energy deprivation promotes decoupling of mitochondrial cytochrome c release from caspase processing and necrotic cell death. Cell Death Differ 2003; 10: 823-32.

Steinbach JP, Wolburg H, Klumpp A, Weller M. Hypoxia sensitizes human malignant glioma cells towards CD95L-induced cell death. J Neurochem 2005; 92: 1340-9.

Takeuchi H, Kondo Y, Fujiwara K, Kanzawa T, Aoki H, Mills GB, et al. Synergistic augmentation of rapamycin-induced autophagy in malignant glioma cells by

phosphatidylinositol 3-kinase/protein kinase B inhibitors. Cancer Res 2005; 65: 3336-46.

Tanaka K, Sasayama T, Mizukawa K, Kawamura A, Kondoh T, Hosoda K, et al. Specific mTOR inhibitor rapamycin enhances cytotoxicity induced by alkylating agent 1-(4-amino-2-methyl-5-pyrimidinyl)methyl-3-(2-chloroethyl)-3-nitrosourea (ACNU) in human U251 malignant glioma cells. J Neurooncol 2007; 84: 233-44.

Thomas GV, Tran C, Mellinghoff IK, Welsbie DS, Chan E, Fueger B, et al. Hypoxia-inducible factor determines sensitivity to inhibitors of mTOR in kidney cancer. Nat Med 2006; 12: 122-7.

Tol J, Koopman M, Rodenburg CJ, Cats A, Creemers GJ, Schrama JG, et al. A randomised phase III study on capecitabine, oxaliplatin and bevacizumab with or without cetuximab in first-line advanced colorectal cancer, the CAIRO2 study of the Dutch Colorectal Cancer Group (DCCG). An interim analysis of toxicity. Ann Oncol 2008; 19: 734-8.

Van Den Bent MJ, Brandes A, Rampling R, Kouwenhoven M, Kros JM, Carpentier AF, et al. Randomized phase II trial of erlotinib (E) versus temozolomide (TMZ) or BCNU in recurrent glioblastoma multiforme (GBM): EORTC 26034. J Clin Oncol (Meeting Abstracts) 2007; 25: 2005.

Wei LH, Su H, Hildebrandt IJ, Phelps ME, Czernin J, Weber WA. Changes in tumor metabolism as readout for Mammalian target of rapamycin kinase inhibition by rapamycin in glioblastoma. Clin Cancer Res 2008; 14: 3416-26.

Weihua Z, Tsan R, Huang WC, Wu Q, Chiu CH, Fidler IJ, et al. Survival of cancer cells is maintained by EGFR independent of its kinase activity. Cancer Cell 2008; 13: 385-93.

Wullschleger S, Loewith R, Hall MN. TOR signaling in growth and metabolism. Cell 2006; 124: 471-84.

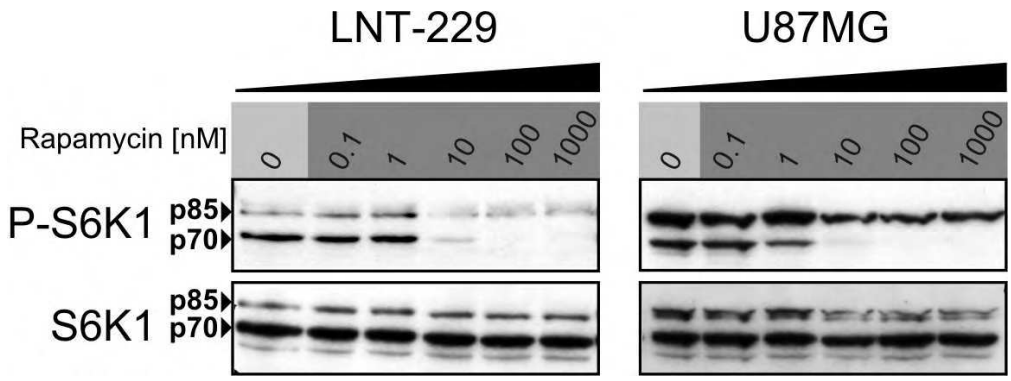

98x35mm (300 x 300 DPI)

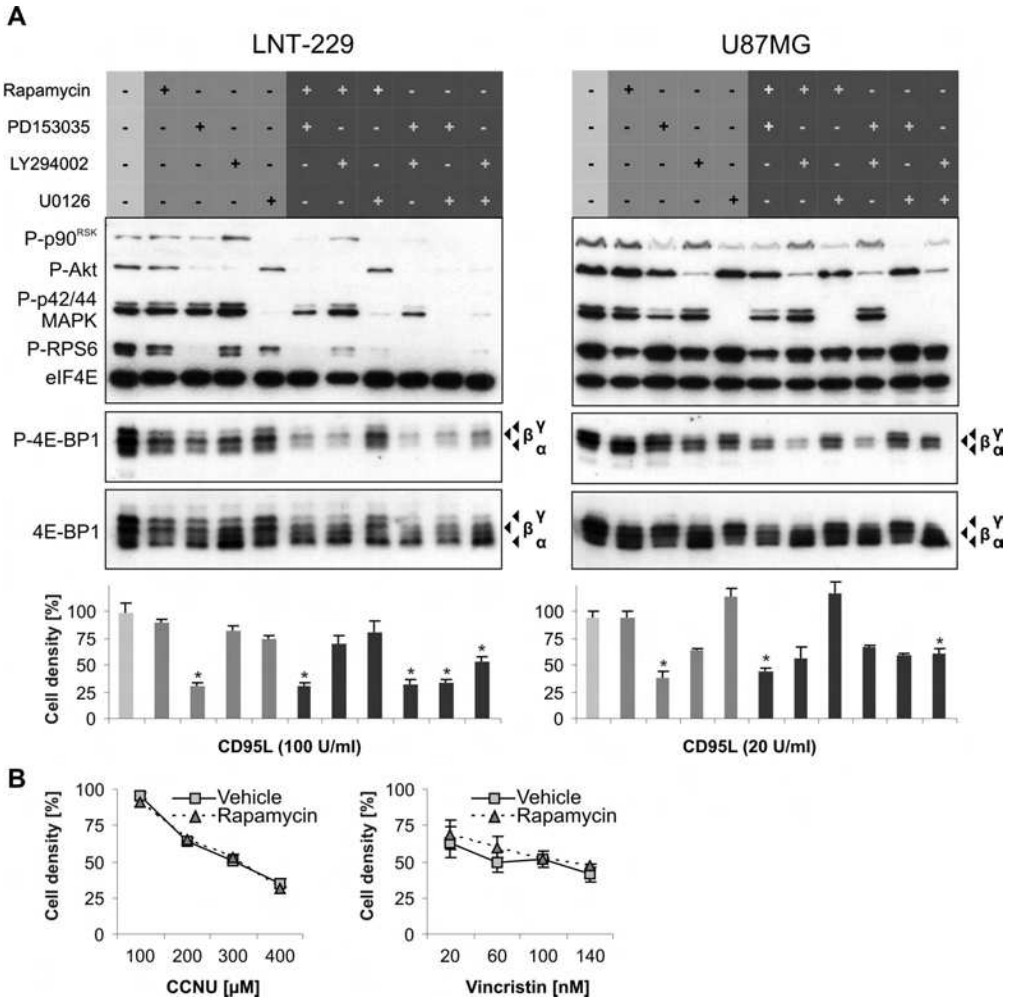

161x159mm (300 x 300 DPI)

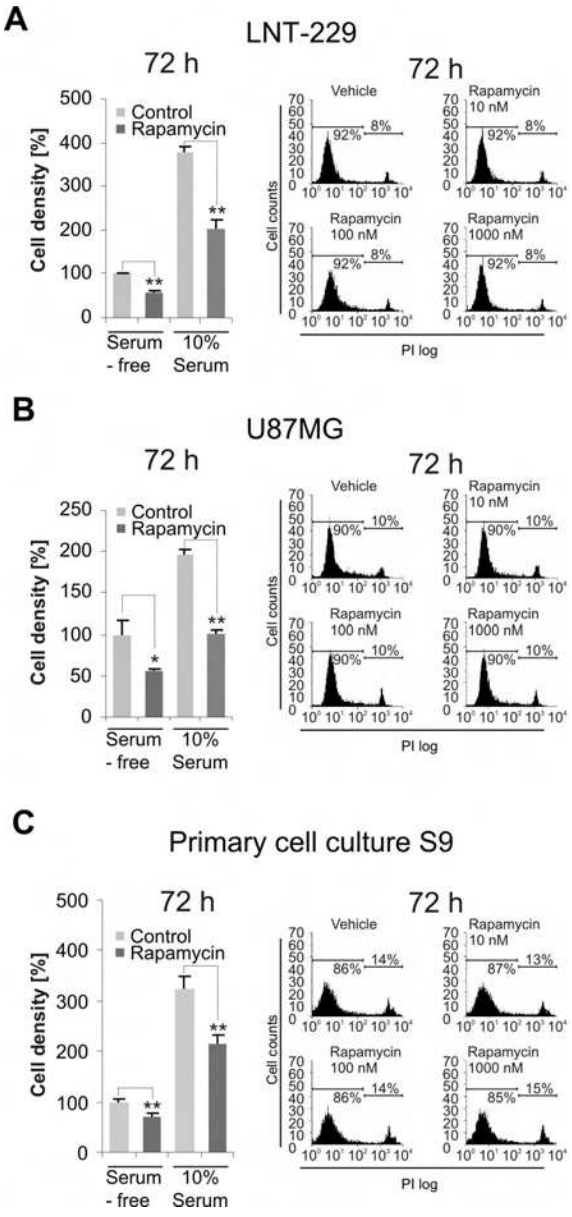

83x177mm (300 x 300 DPI)

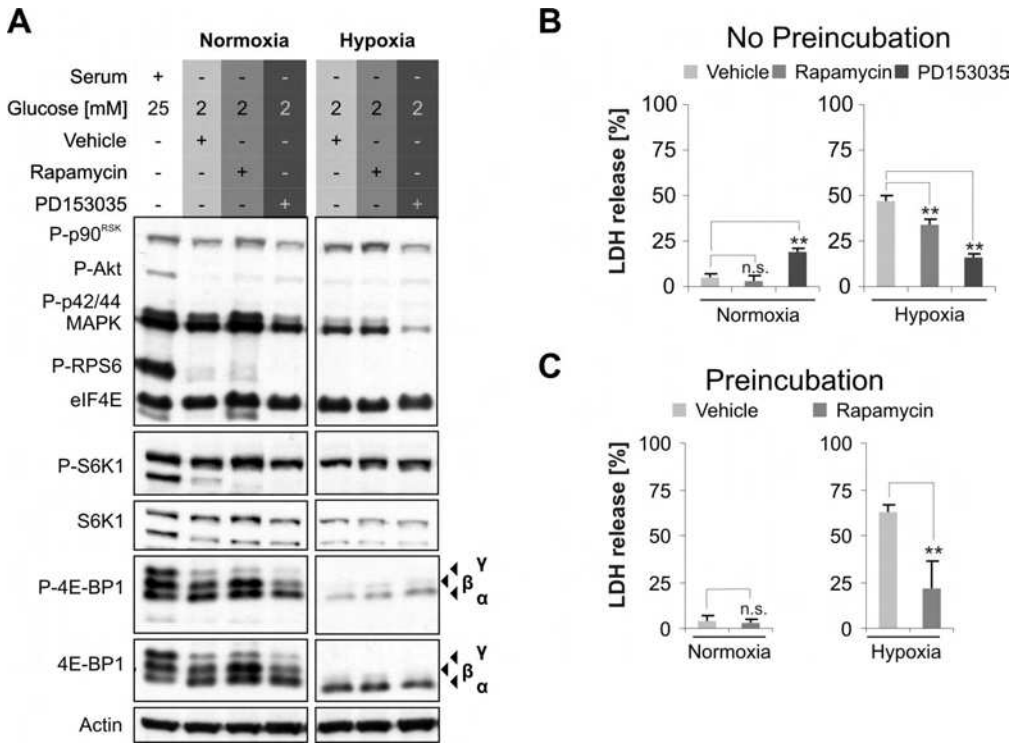

144x106mm (300 x 300 DPI)

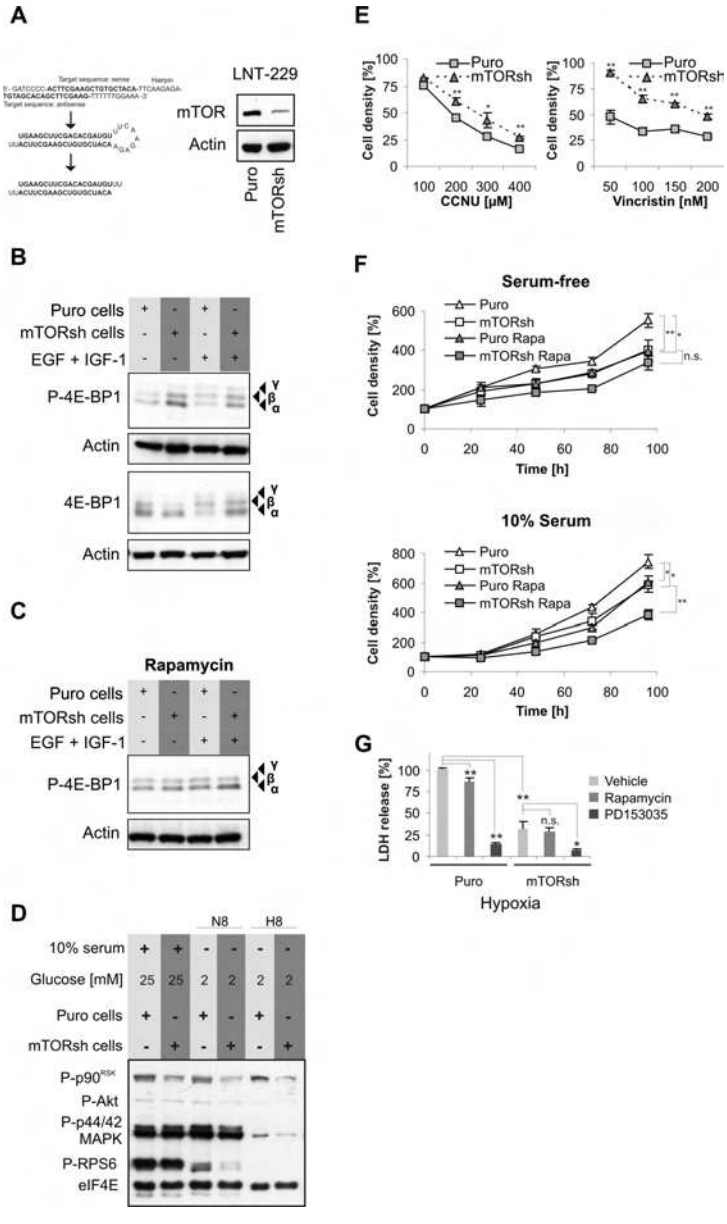

151x252mm (300 x 300 DPI)

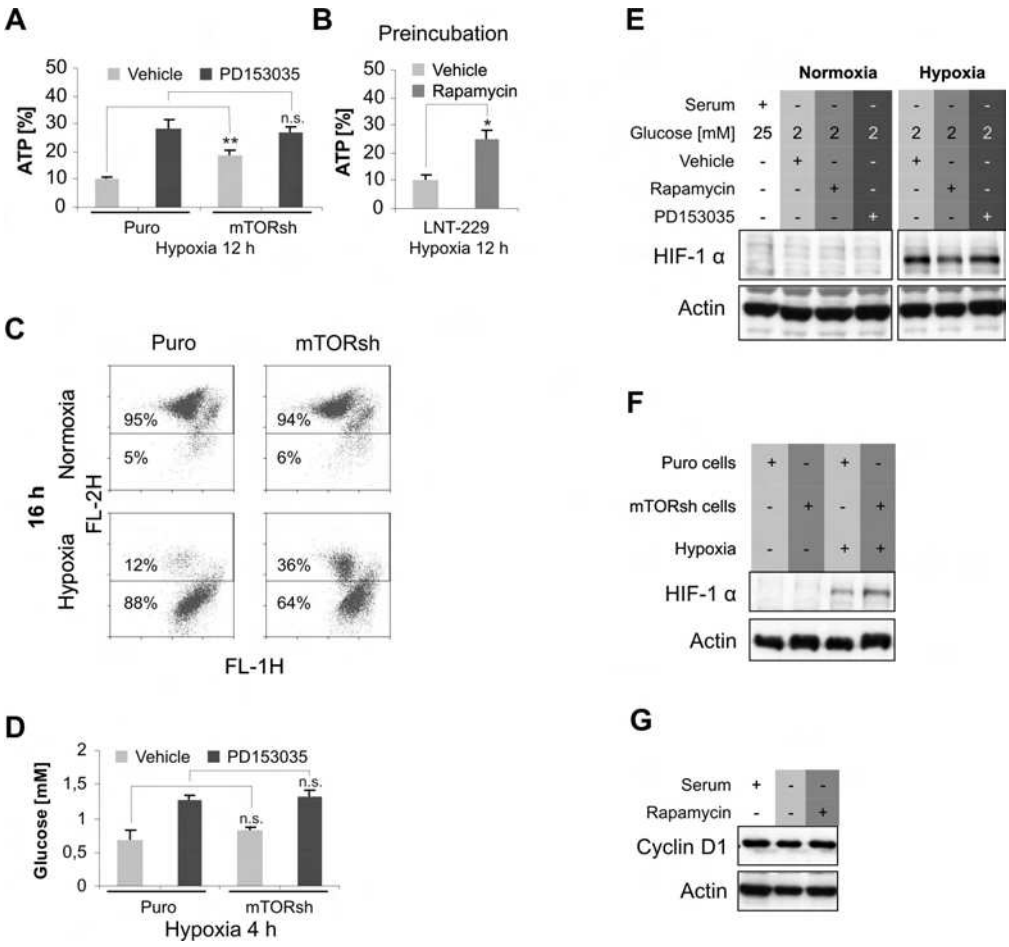

165x154mm (300 x 300 DPI)

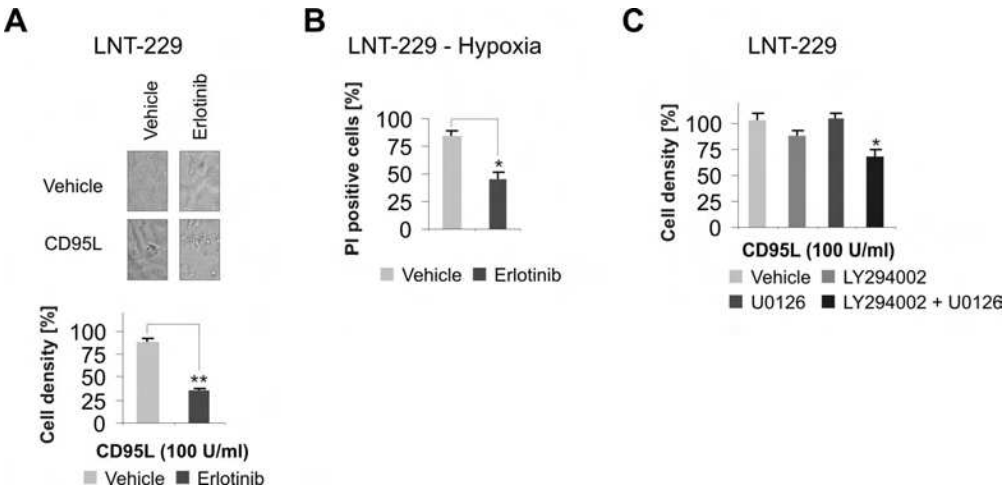

151x72mm (300 x 300 DPI)

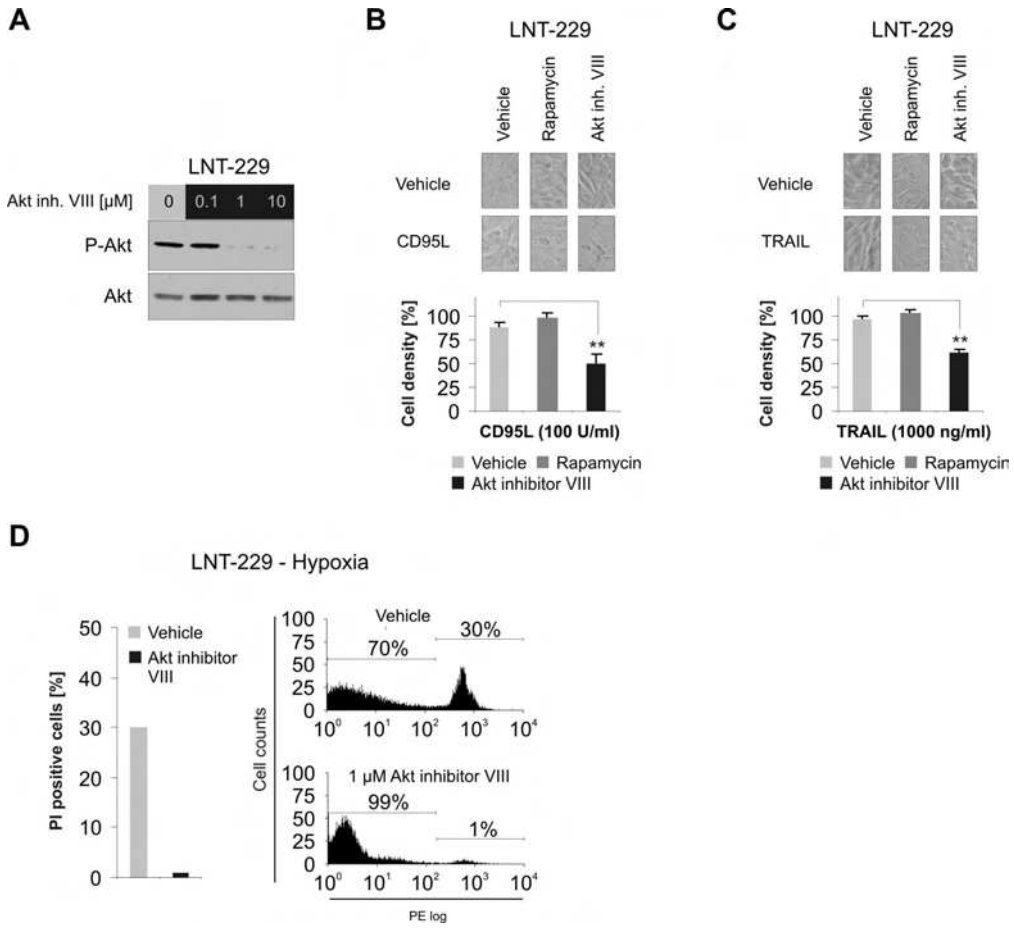

165x150mm (300 x 300 DPI)

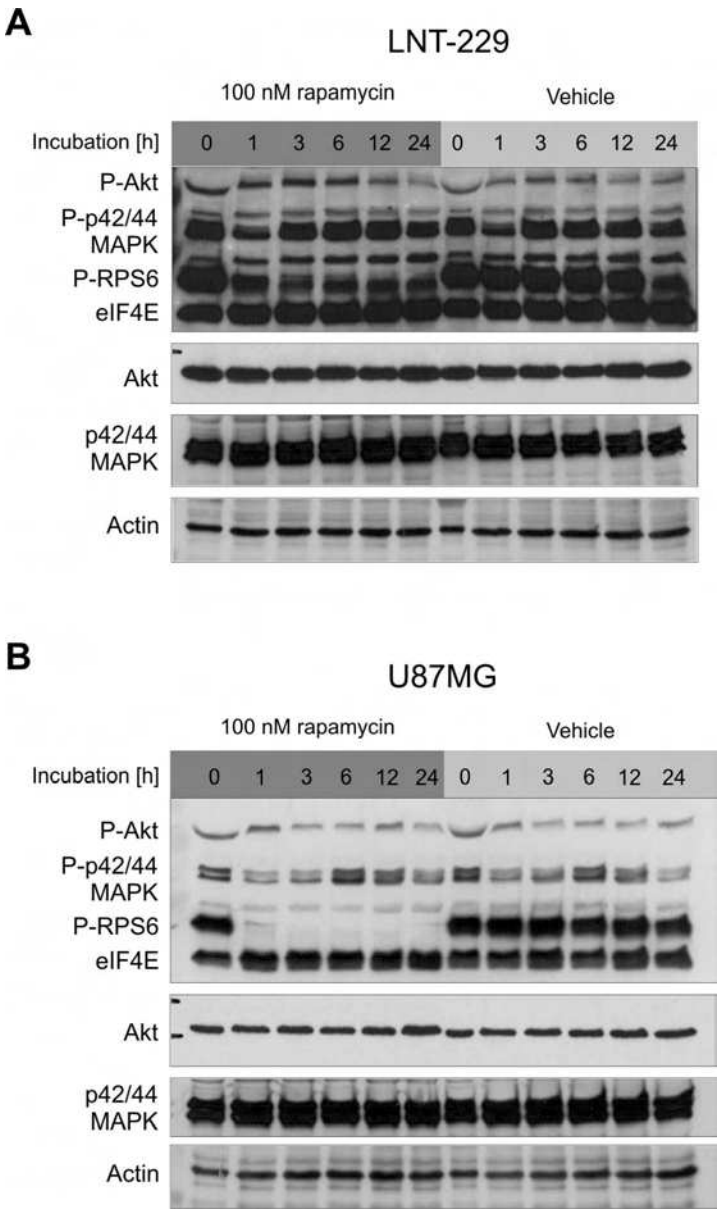

94x158mm (300 x 300 DPI)

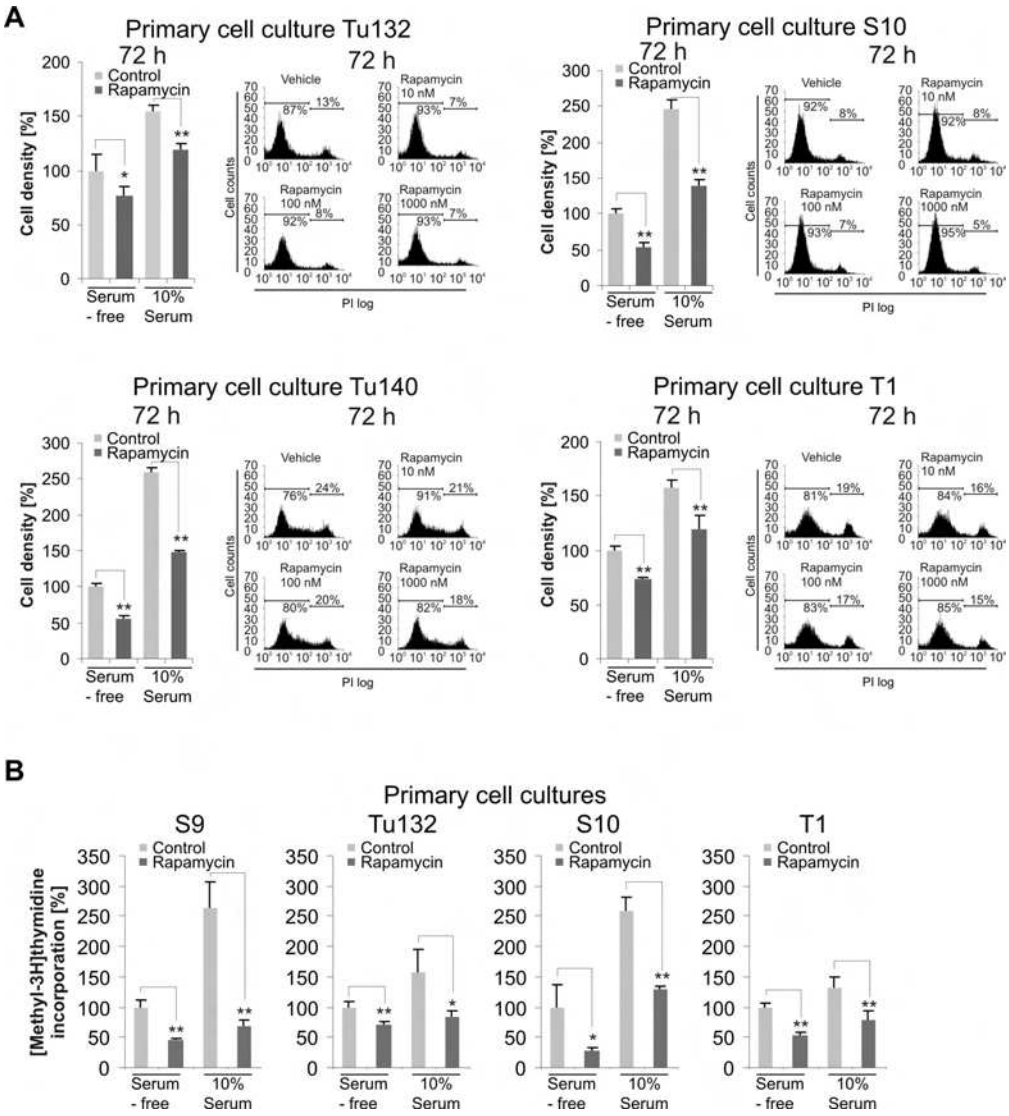

171x188mm (300 x 300 DPI)

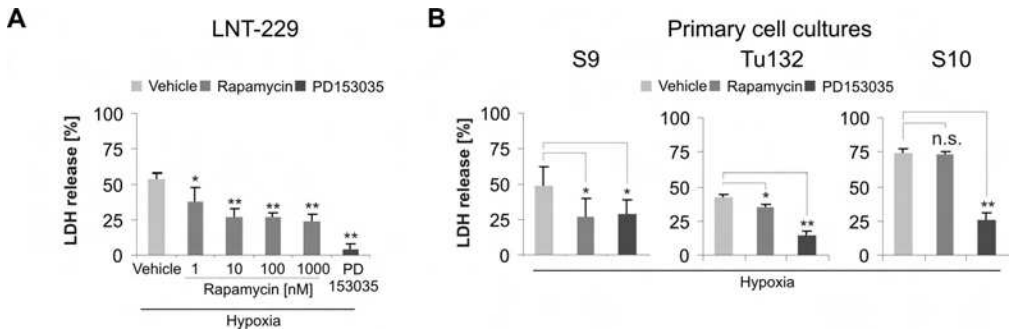

186x59mm (300 x 300 DPI)

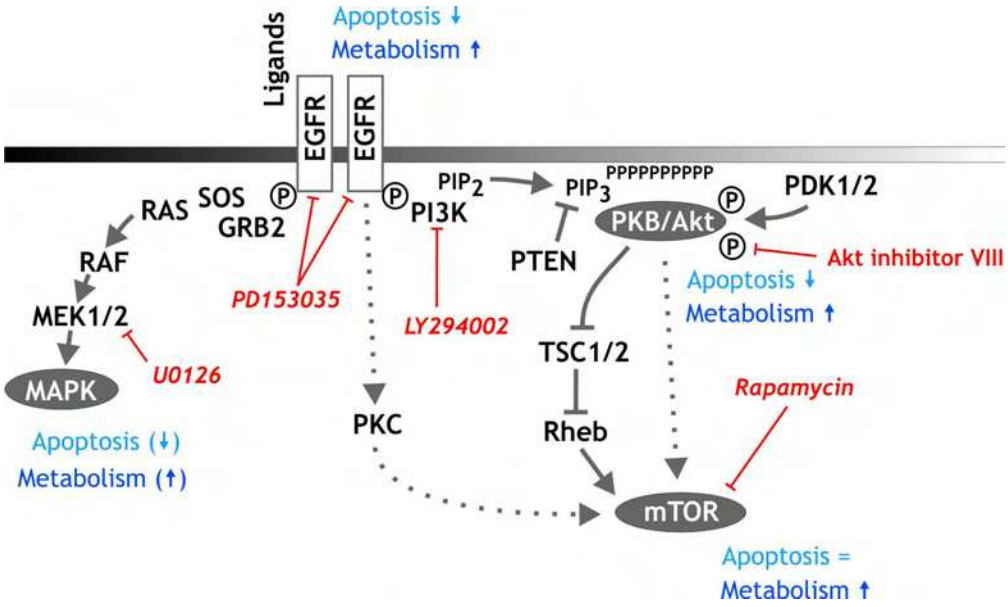

153x90mm (300 x 300 DPI)